

INIS-ref. - 6572

INIS DOCUMENT

TRN IL8102201 -

IL8102282;

IL8102285 -

IL8102289

# Bulletin of

THE

ISRAEL

PHYSICAL

SOCIETY

BULLETIN of the IPS, Vol. 26, 1980



WEIZMANN  
INSTITUTE  
OF SCIENCE

1980

ANNUAL MEETING

PROGRAM

AND

ABSTRACTS

# **Bulletin of**

**THE**

**ISRAEL**

**PHYSICAL**

**SOCIETY**



**WEIZMANN  
INSTITUTE  
OF SCIENCE**

**1980**

**ANNUAL MEETING**

**PROGRAM**

**AND**

**ABSTRACTS**

האגודה הישראלית לפיסיקה

רשימת חברי הוועד לשנת 1980 - 1979

אוניברסיטת בר-אילן, רמת גן	מ. לובן	נשיא
אוניברסיטת בן-גוריון, באר שבע	מ. כרמלי	סגן-נשיא
מרכז למחקר גרעיני, נחל שורק	ב. ארד	גזבר
אוניברסיטת בר-אילן, רמת גן	י. שלזינגר	מזכיר
משרד הבטחון	מ. מנת	חברים
קריה למחקר גרעיני, באר שבע	ע. עצמוני	
האוניברסיטה העברית, ירושלים	ב.ז. פרנקל	
מכון ויצמן למדע, רחובות	מ. קוגלר	
הטכניון, מכון טכנולוגי לישראל, חיפה	צ'. קוטר	
אוניברסיטת חל אביב, רמת אביב	ס. קורמן	

**THE ISRAEL PHYSICAL SOCIETY**

**1980 ANNUAL MEETING**

**Wednesday, April 9 - Thursday, April 10, 1980**

**WEIZMANN INSTITUTE OF SCIENCE, REHOVOT**

**General Information**

The 1980 annual meeting of the Israel Physical Society will take place at the Weizmann Institute of Science on Wednesday, April 9th and Thursday April 10th, 1980.

Registration will begin at 9:00 a.m. on Wednesday in the Wix Auditorium. On Thursday morning between 08:30 a.m.-10:30 a.m. there will be registration desks at the entrance of the Feinberg Graduate School and the Nuclear Physics building.

The plenary sessions will take place in the Wix Auditorium and the parallel sessions will be held in the Nuclear Physics building and the Feinberg Graduate School.

The organizing committee is grateful to the Weizmann Institute of Science for its help in the organization of this meeting.

**The Organizing Committee**

**M. Milgrom - Chairman**  
**S. Gurvitz**  
**M. Hass**  
**D. Mukamel**  
**E.E. Ronat**

**THE ISRAEL PHYSICAL SOCIETY**

**1980 ANNUAL MEETING**

**Wednesday, 9th April - Thursday, 10th April**

**The Weizmann Institute of Science, Rehovot.**

**CONDENSED PROGRAM**

**Wednesday Morning**

**Wix Auditorium**

**9:00 REGISTRATION**

**10:00 OPENING SESSION**

**M. Luban, Bar Ilan University - Presiding**

**WORDS OF WELCOME**

**I. Talmi, Dean of the Faculty of Physics,  
Weizmann Institute of Science**

**Presentation of the Yom-Kippur War Memorial Fund  
Scholarships, granted by the IPS in memory of members  
of the Society killed in the Yom-Kippur War**

**10:30 PLENARY SESSION I**

**I. Dostrovsky, Weizmann Institute of Science**

**SOLAR NEUTRINO EXPERIMENTS**

**(40 min.)**

**C O F F E E   B R E A K**

**N. Rosen, Technion, Israel Institute of Technology-Haifa**

**DO BLACK HOLES EXIST ?**

**(40 min.)**

**12:30 BUSINESS MEETING OF THE ISRAEL PHYSICAL SOCIETY**

**13:30**

**L U N C H**

**San Martin**

Wednesday Afternoon

14:30 Parallel Sessions

A. NUCLEAR PHYSICS

Phys. Bldg.  
Large Lect.  
Hall

E. Fridman - Presiding

J. Alster, The Tel Aviv University (25 min.)  
Neutron and Proton Radii from Pion  
Elastic Scattering

Contributed Papers

I. Tserruya, The Weizmann Institute (25 min.)  
Heavy Ion Reactions

Contributed Papers

B. ASTROPHYSICS AND RELATIVITY

Phys. Bldg.  
Small Lect.  
Hall

E. Leibowitz - Presiding

Y. Avni, The Weizmann Institute (25 min.)  
The Einstein (HEAO-2) X-ray Observatory:  
First Results

Contributed Papers

J. Shaham, The Hebrew University (25 min.)  
Observational Evidences for Neutron Stars  
and Black Holes

Contributed Papers

C. METALS AND CONDUCTIVITY

Feinberg A

N. Wiser - Presiding

E. Ehrenfreund, Technion IIT (25 min.)  
Electronic Properties of Pure and Doped  
Polyacetylene

Contributed Papers

B. Horowitz, The Weizmann Institute (25 min.)  
Conductivity in Charge-Density-Wave  
Systems

Contributed Papers

**D. OPTICS AND LASERS Feinberg B**

**I. Smilansky - Presiding**

**A. Hardy, The Weizmann Institute (25 min.)  
Laser Resonators with Phase-Conjugate  
Mirrors**

**Contributed Papers**

**E. PLASMA PHYSICS I Feinberg D**

**B.S. Frenkel - Presiding**

**Z. Zinamon, The Weizmann Institute (25 min.)  
Interaction of Intense Particle Beams  
with Matter**

**Contributed Papers**

**Thursday Morning**

**08:30 - 10:00 Registration (Feinberg or Physics Bldgs.)**

**09:00 Parallel Sessions**

**F. PHASE TRANSITIONS AND INSTABILITIES Feinberg A**

**S. Alexander - Presiding**

**A. Ron, Technion, IIT. (25 min.)  
Ferromagnetic Superconductors**

**Contributed Papers**

**G. PLASMA PHYSICS II Feinberg D**

**D. Salzmann - Presiding**

**E. Shalom, Soreq Nuclear Research Center (25 min.)  
Wave Phenomena in Laser Fusion**

**H. THIN FILMS Phys. Bldg.  
Large Lect.  
Hall**

**G. Deutcher - Presiding**

**U. Admon, Nuclear Research Center (25 min.)  
The Morphology, Phase Constitution  
and Texture of Polycrystalline Thin  
Films**

**Contributed Papers**

**J. Shamir, Technion, IIT (25 min.)  
Optical Analysis of Thin Films**

**Contributed Papers**

**BUSINESS MEETING**

I. SEMICONDUCTORS AND MAGNETISM

Feinberg B

H. Shaked - Presiding

Contributed Papers

E. Gurewitz, Nuclear Research Center (25 min.)  
Anisotropic Spin Glass Behavior in  $\text{Fe}_2\text{TiO}_5$

Contributed Papers

J. ATOMS AND MOLECULES

Phys. Bldg.  
Small Lect.  
Hall

B. Rosner - Presiding

S. Yatsiv, The Hebrew University (25 min.)  
Recombination Spectrum of High Pressure  
Xenon and Argon with Hg Vapor

Contributed papers

K. APPLIED PHYSICS

Feinberg C

G. Yekutieli - Presiding

Contributed Papers

12:30 Concert - Baroque Music:

Wix Auditorium

Christopher Sarr - Harpsichord

Gerdien Tanja - Recorder

13:30 L U N C H

San Martin

Thursday Afternoon

14:30 PLENARY SESSION II

Wix Auditorium

G. Goldring - Presiding

T. Banks, The Tel Aviv University

UNIFIED THEORIES OF ELEMENTARY PARTICLE INTERACTIONS (40 min.)

COFFEE BREAK

E. Kogan, Tadiran Electronics Division, Holon

SURFACE ACOUSTIC WAVES TECHNOLOGY AND ITS APPLICATIONS  
TO SIGNAL PROCESSING IN COMMUNICATION SYSTEMS (40 min.)



THE ISRAEL PHYSICAL SOCIETY  
1980 ANNUAL MEETING

Wednesday, 9th April - Thursday, 10th April  
The Weizmann Institute of Science, Rehovot.

COMPLETE PROGRAM

Wednesday Morning

Wix Auditorium

9:00 REGISTRATION

10:00 OPENING SESSION

M. Luban, Bar Ilan University - Presiding

WORDS OF WELCOME

I. Talmi, Dean of the Faculty of Physics,  
Weizmann Institute of Science

Presentation of the Yom-Kippur War Memorial Fund  
Scholarships, granted by the IPS in memory of members  
of the Society killed in the Yom-Kippur War

10:30 PLENARY SESSION I

I. Dostrovsky, Weizmann Institute of Science

SOLAR NEUTRINO EXPERIMENTS (40 min.)

COFFEE BREAK

N. Rosen, Technion, Israel Institute of Technology-Haifa

DO BLACK HOLES EXIST ? (40 min.)

12:30 BUSINESS MEETING OF THE ISRAEL PHYSICAL SOCIETY

13:30

LUNCH

San Martin

WEDNESDAY AFTERNOON, APRIL 9, 1980  
14:30

Phys. Bldg.  
Large. Lect.  
Hall

## A. NUCLEAR PHYSICS

E. FRIDMAN, The Hebrew University of Jerusalem - Presiding

### A-1 INVITED

NEUTRON AND PROTON RADII FROM PION ELASTIC SCATTERING

J. Alster, The Tel Aviv University

### A - 2

SCATTERING THEORY FOR THE COUPLED  $\pi NN$ - $NN$  SYSTEMS

Y. Avishai, Ben Gurion University, Beer Sheva, Israel

T. Mizutani, IPN, F91406 Orsay Cedex, France

The theory of coupled  $\pi NN$ - $NN$  systems incorporates two distinct physical phenomena, namely inelastic  $NN$  scattering and the effect of true pion absorption on elastic  $\pi d$  scattering. We have investigated this system and derived coupled equations for all the pertinent physical amplitudes. Later on, we have extended the results to include relativity<sup>1</sup> and the numerical solution of these modified equations is now under way. Yet, some peculiar obstacles arise when the  $\pi N$  interaction in the  $P_{11}$  state gets its contribution from both the dressed nucleon pole term as well as a non pole part. In this note we report on the derivation of equations which incorporate the two contributions mentioned above, and hence they are appropriate for studying problems with  $T_{lab} > 100$  MeV where the pole term alone is insufficient. The equations are obtained either by the irreducibility arguments of Taylor<sup>2</sup> or simply by adding the non-pole term to the equations of Ref. 1. In these new equations the  $\pi NN$  vertices and the two nucleon propagator are fully dressed with both pole and non-pole contributions.

1. Y. Avishai and T. Mizutani Nucl. Phys. A326 (1979) 352 and in press.
2. J.G. Taylor Phys. Rev. 150A (1966)1321.

A - 3

## THEORY OF LARGE ANGLE p-NUCLEUS SCATTERING.

I. pd ELASTIC SCATTERING AND DEUTERON FORM FACTOR AT LARGE  $q^2$ .

S.A. Gurvitz

Department of Nuclear Physics, Weizmann Institute of Science,  
Rehovot

We derived a new approach to the proton-nucleus large angle scattering which accounts in a systematic way for Pauli, binding, and Fermi motion effects<sup>1</sup>). We concentrated here on pd scattering. After antisymmetrization of incident and target protons (which has been done without any approximations), the pd amplitude has been found as a sum of two components<sup>2</sup>). The first one is the modified multiple scattering series and the second one is distorted neutron pick up amplitude. The optimal approximation<sup>3</sup>) designed to minimize corrections has been derived for the antisymmetrized pd amplitude. The single scattering amplitude has been obtained to be factorized into an on-shell (antisymmetrized) pN amplitude and the deuteron form factor and it has been found to play a main role in the large angle pd scattering at sufficiently high energy. These results were applied to analysis of pd elastic scattering data ( $T_p \gtrsim 300$  MeV) which has been found well reproduced by the calculations. This analysis also permits an extraction of the deuteron body form factor for values  $q^2$  which far exceed those measured in ed elastic data<sup>4</sup>). Therefore using our approach the large angle pd data could be used as a source of information on the deuteron form factor at large  $q^2$ .

1. S.A. Gurvitz, Phys. Rev. C, in print.
2. S.A. Gurvitz, Phys. Rev. Lett. Sub. for publication
3. S.A. Gurvitz, J.-P. Dedonder and R.A. Amado, Phys. Rev. C19, 142 (1979); S.A. Gurvitz, Phys. Rev. C20, 1256 (1979).
4. R. Arnold et al., Phys. Rev. Lett. 35, 776 (1975).

A - 4ASYMPTOTIC NORMALIZATION OF THE  $\alpha$ -tp,  $\alpha$ -tn AND  $\tau$ -dp FROM CHARGE FORM FACTOR PARAMETRIZATION.

A. Moalem and S. Rozenfeld

Department of Physics, Ben-Gurion University, Beer-Sheva, Israel

The normalization constants for DWBA calculations of single particle transfers of the type  $A+a \rightarrow (A+N) + b$  is closely related to  $C$ , the asymptotic normalization of the  $a$ -bN overlap function  $R(\rho)$  and can be determined from dispersion relations analysis of scattering data<sup>1</sup>, from charge form factor parametrization<sup>2</sup> and from transfer relation data<sup>3</sup>. In a recent publication<sup>3</sup> we have indicated that the scatter in values of  $C^2$  for the  $\alpha$ -tp,  $\alpha$ -tn and  $\tau$ -dp from these three sources is a bit too large compared to the

accuracy attributed to the various sources of information. Therefore we have reexamined the available experimental charge form factors for  $^3\text{He}$  and  $^4\text{He}$ . Our analysis yields  $C^2 = 13.6, 12.4$  and  $3.1$  for the  $\alpha$ -tp,  $\alpha$ -rn and  $\tau$ -dp respectively. These values differ slightly from those of  $\text{Lim}^2$  but are in a better agreement with the values from transfer reaction data<sup>3</sup>. The values quoted above agree well with dispersion relation results which take into account Coulomb effects<sup>1</sup>.

### References

1. M.P. Locher and T. Mizutani, Phys. Reports 46, 43 (1978).
2. T.K. Lim, Phys. Lett. 44B, 341 (1973); 55B, 252 (1975) and references therein.
3. A. Moalem and Z. Vardi, Nucl. Phys. A332, 205 (1979).

### A - 5

#### DE-EXCITATION MODES OF LOW LYING LEVEL IN $^{128}\text{I}$ FROM THE $^{128}\text{Te}(p,n\gamma)^{128}\text{I}$ REACTION

J. Burde, V. Richter, I. Labaton  
Racah Institute of Physics, The Hebrew University, Jerusalem,  
Israel

A. Moalem  
Physics Department, Ben-Gurion University of the Negev,  
Beer-Sheva, Israel

As part of a broader programme to elucidate the level structure of the odd-odd iodine isotopes we report herein on the results from a study of the  $^{128}\text{Te}(p,n\gamma)^{128}\text{I}$  reaction in the energy range  $E_p=2.8$  to 5.0 MeV. Singles gamma spectra and gamma-gamma coincidence yields were measured using high resolution three parameters Ge(Li)-Ge(Li)-timing system<sup>1</sup>). A level scheme which includes 41 excited states was constructed and upper limits were placed on the lifetime of six levels. Angular distributions combined with the results from coincidence measurements and the population strength of the states by primaries in the  $(n,\gamma)$  reaction<sup>2</sup>) enabled us to make a spin and parity assignment for many states. The decay modes of many levels as obtained in the present work are different from those proposed in the  $(n,\gamma)$  study. The ground states ( $1^+$ ) and the positive parity states: 27.4 ( $2^+$ ), 85.5 ( $3^+$ ), 151.6 ( $3^+$ ), 160.6 ( $2^+$ ), 232.6 ( $4^+$ ), 295.6 ( $3^+$ ), 481.4 ( $5^+$ ), 613 ( $4^+$ ) and 678 keV ( $4^+$ ) are described in terms of admixed two quasi-particle multiplets. Good agreement was attained between the experimental and theoretical values of 29 gamma intensity branching ratios that comprised all the conceivable M1 and E2 transitions between these states. Some negative parity states are assigned as members of the  $|\pi 9/2^-\nu h_{11/2}^-\rangle$  and the  $|\pi d_{5/2}^-\nu h_{11/2}^-\rangle$  two quasi-particle multiplets.

- 1) J.Burde, V.Richter, I.Labaton, A.Moalem and D.Kalinsky, Nucl. Inst. and Meth. 151 (1978) 261.
- 2) L.A.Schaller, J.Kern and B.Michaud, Nucl. Phys. A165 (1971)415.

A - 6STUDY OF INTERFERENCE BETWEEN GIANT RESONANCES  
VIA THE  $^{206,207}\text{Pb}(\gamma, n)$  REACTION.

Y. Birenbaum, Z. Berant, S. Kahane, R. Moreh\* A. Wolf  
Nuclear Research Center-Negev, Beer-Sheva

Measurement of angular distributions of neutrons from the  $(\gamma, n)$  reaction is used as a tool for investigating the existence of interference between E1, E2, M1 multipoles in the entrance channel. We used monoenergetic gamma rays in the range  $E_\gamma=7-11.4\text{MeV}$ , produced by thermal neutron capture in nickel and chromium discs placed near the core of the IRR-2 reactor. The neutrons were detected in a high resolution (30keV FWHM at 1 MeV)  $^3\text{He}$  spectrometer. Natural and isotopically enriched lead targets were used.

In addition to previously published<sup>(1)</sup> results for  $^{206}\text{Pb}(\gamma, n)$ , new data for  $^{207}\text{Pb}(\gamma, n)$  is presented. In several cases, a pronounced asymmetry around  $90^\circ$  is observed, indicating the existence of E1-E2 and maybe also E1-M1 interference. The results are compared with theoretical calculations based on the direct-semidirect model<sup>(2)</sup>. These calculations were performed for several final states in the  $^{205,206}\text{Pb}$  residual nuclei.

1. Y. Birenbaum, Z. Berant, A. Wolf and R. Moreh, Phys. Letters 88B, 239 (1979).
2. C.F. Clement, A.M. Lane and J.R. Rook, Nucl. Phys. 66, 273 (1965).

\* On sabbatical at the University of Illinois at Urbana-Champaign.

A - 7 INVITED

## HEAVY ION REACTIONS

I. Tserruya, The Weizmann Institute of Science

A - 8LINEAR RESPONSE RPA CALCULATIONS FOR  $^{16}\text{O}$  and  $^{18}\text{O}$ 

A. Moalem and J. Bar-Touv

Department of Physics, Ben-Gurion University, Beer-Sheva, Israel

In a recent publication<sup>1)</sup>, a procedure was presented which allows the application of linear response Theory and Random Phase Approximation (RPA) to open shell spherical nuclei. An essential feature of this procedure was the introduction of occupation parameters  $\Theta_{nlj}$  in the early stage of determining the single particle basis. Such occupation numbers were also incorporated in the Tensor Open Shell RPA (TOSRPA) method<sup>2)</sup>. However unlike the TOSRPA our model is exactly soluable and maintains the simplicity of the linear response methods. In both methods the true ground state is approximated by the ground state of a preliminary shell model or projected HF calculations. Our main interest in the present contribution was to examine the effects of a given ground state description on the characteristics of collective states in  $^{16}\text{O}$  and  $^{18}\text{O}$ . Wave functions which assume closed  $^{16}\text{O}$  and the more elaborate shell model wave functions of ref.<sup>3)</sup> were used to describe the ground state. Our findings are as follows: (1) Collective states and multipole giant resonances which were predicted with the simple wave functions are also reproduced by the more elaborate wave functions. (2) With the wave functions based on  $^{12}\text{C}$  core rather than  $^{16}\text{O}$  the response was more structured particularly in the low energy region. (3) The general properties of multipole giant resonances varied rather slightly. Finally the properties of giant multipole resonances exhibit strong shell effects in accord with the available data.

References

- 1) J. Bar Touv, A. Moalem and S. Shlomo, in press in Nucl. Phys. A.
- 2) C. Ngo-Trong, T. Suzuki and D.J. Rowe, Nucl. Phys. A313 (1979) 15.
- 3) A.P. Zuker, Phys. Rev. Lett. 23 (1969) 983.

A - 9MAGNETIC MOMENTS IN NUCLEI NEAR CLOSED SHELL: THE  $2_1^+$  LEVELS IN EVEN Zr and Sn ISOTOPES

M. Hass, C. Broude, Y. Niv and A. Zemel

Department of Nuclear Physics, Weizmann Institute of Science, Rehovot

The g-factors of the  $2_1^+$  levels of even Zr and Sn isotopes have been measured using the dynamic (transient) magnetic field which acts on nuclei in fast ions traversing a thin magnetized iron foil. The thin foil dynamic field technique has been described in numerous recent publications and its advantages in magnetic moment measurements of ps nuclear level have been amply demonstrated<sup>(1)</sup>

The experiments were carried out at the Pelletron accelerator of the Weizmann Institute using beams of 90 MeV and 108 MeV of  $^{35}\text{Cl}$  ions to Coulomb excite the  $2^+_1$  levels. The results obtained are:  $g=+.37(13)$ ,  $g=0$ ,  $g=-.16(10)$ ,  $g=+.02(9)$ ,  $g=-.14(7)$ ,  $g=-.07(11)$  and  $g=-.15(10)$  for  $^{112-124}\text{Sn}$ , respectively and  $g=-.03(5)$  and  $g=-.26(6)$  for  $^{92,94}\text{Zr}$ , respectively. The Sn results demonstrate the closure of the  $Z=50$  shell and the sensitivity of the measurement to the occupation parameters of the various single-particle neutron configurations in this mass region. The Zr results indicate sizeable admixtures of components other than  $d_{5/2}$  neutrons in the wave functions of these levels. The significance of the present results regarding the shell-model composition of the corresponding wave functions will be discussed.

(1) M. Hass, N. Benczer-Koller, J.M. Brennan, H.T. King and P. Goode, Phys. Rev. C17, 947 (1978); and references therein.

## A - 10

### g FACTOR OF THE FIRST EXCITED $2^+$ STATE IN $^{100}\text{Zr}$ .

A. Wolf  
Nuclear Research Center-Negev, Beer-Sheva

G. Battistuzzi, K. Kawade, H. Lawin and K. Sistemich  
KFA Julich, F.R. of Germany

Energy level systematics of the Zr isotopes exhibit a clear shape transition as a function of neutron number. This transition takes place at  $N=60$  (i.e.,  $^{100}\text{Zr}$ ). The first excited  $0^+$  state drops drastically from 0.85 MeV in  $^{98}\text{Zr}$ , to only 0.33 MeV in  $^{100}\text{Zr}$ . A similar drop occurs for the first excited  $2^+$  state. We measured the g-factor of the  $2^+_1$  state in  $^{100}\text{Zr}$  ( $t_{1/2}=0.71$  nsec), using the integral perturbed angular correlation technique for the  $0^+_1 \rightarrow 2^+_1 \rightarrow 0^+_1$  cascade (1).  $^{100}\text{Zr}$  was obtained from  $\beta$ -decay of  $^{100}\text{Y}$  at the fission product on-line separator JOSEF at the KFA, Julich. Three Ge(11) detectors were used, at angles of  $30^\circ$  and  $150^\circ$  with each other. An external static magnetic field of 31.5 kGauss was applied.

The result,  $g=0.24 \pm 0.05$ , indicates a rotational structure for the first excited  $2^+$  state in  $^{100}\text{Zr}$ .

1. H. Selic et al., Z. Phys. A286, 123 (1978).

A - 11

## NUCLEAR ANTI-STOKES TRANSITIONS INDUCED BY LASER RADIATION

B. Arad, S. Eliezer and Y. Paiss, Soreq Nuclear Research Center, Yavne 70600, Israel

We are suggesting that the lifetime of a nuclear transition can be significantly changed by using laser photons which have wavelength 5 to 6 order of magnitude larger than the induced nuclear transitions. In order to calculate the cross-section for this phenomenon we start with a nuclear isomeric level which decays naturally via an EIII transition. The enhancement is induced by the laser photon transforming the one step EIII transition into a two step EI, EII transition taking place through a "virtual" state. The "virtual" state is a far out Breit-Wigner tail of a real nuclear level. In order to calculate the cross-section we have used the theoretical single particle Weisskopf transition probability rates corrected by the experimental  $M/2$  values.

In order to test the validity of such a case  $^{111m}\text{Pd}$  was chosen and the cross-section was calculated following the procedure outlined here.

A - 12RESONANT SCATTERING OF GAMMA RAYS FROM  $^{62}\text{Ni}$  IN  $\text{Mg}_2\text{Ni}$ ,  $\text{Mg}_2\text{NiH}$ , AND  $\text{Mg}_2\text{NiD}$ .

I. Jacob, M.H. Mintz, O. Shahal\* and A. Wolf  
Nuclear Research Center-Negev, Beer-Sheva

The temperature dependence of the resonance scattering cross section  $\sigma_R$  of 7.646 MeV photons from  $^{62}\text{Ni}$  in  $\text{Mg}_2\text{Ni}$ ,  $\text{Mg}_2\text{NiH}$ , and  $\text{Mg}_2\text{NiD}$ , was measured in the range  $80^\circ\text{K} - 300^\circ\text{K}$ . The photon beam was obtained from the  $(n,\gamma)$  reaction in iron discs placed near the core of the IRR-2 reactor. The temperature effect, defined as  $\sigma_R(80^\circ\text{K})/\sigma_R(300^\circ\text{K})$  was found to be  $0.901 \pm 0.007$ ,  $0.915 \pm 0.005$ ,  $0.924 \pm 0.005$  for  $\text{Mg}_2\text{Ni}$ ,  $\text{Mg}_2\text{NiH}$ , and  $\text{Mg}_2\text{NiD}$ , respectively.

From the values of the temperature effect, and using the known [1] nuclear parameters ( $\Gamma_0, \Gamma$ ) of the 7.646 MeV level in  $^{62}\text{Ni}$ , the Debye temperatures for the three compounds were calculated. The results clearly indicate an increase of the Debye temperature after hydrogenation or deuterization.

1. R. Moreh, O. Shahal and I. Jacob, Nucl. Phys. A228, 77 (1974).

\*On sabbatical leave at Oak Ridge National Laboratory



WEDNESDAY AFTERNOON, APRIL 9, 1980  
14:30

PHYSICS BLDG.  
SMALL LECT.  
HALL

## B. ASTROPHYSICS AND RELATIVITY

E. Leibowitz, The Tel Aviv University - Presiding

### B - 1 INVITED

THE EINSTEIN (HEAO-2) X-RAY OBSERVATORY: FIRST RESULTS.

Y. Avni, The Weizmann Institute, Rehovot

### B - 2

EJECTIONS OF MATTER AND ENHANCED ELECTROMAGNETIC RADIATION IN  
THE SOLAR ATMOSPHERE

Varda Bar  
Tel Aviv University, School of Education

There are some instances of transient phenomena in the solar atmosphere in which ejections of matter and enhanced electromagnetic (EM) radiation are related. They are: Spicules, Macro spicules, Short surges and Long surges. Those phenomena are different from each other in the order of magnitude of their intensity but they are similar in various characteristics:

1. Enhanced EM radiation and ejections of matter can be observed in all of them.
  2. The ejections are observed as black streams on the disk and red when exposed on the solar limb.
  3. They are situated in locations where magnetic fields of opposite polarities are close to each other.
  4. Those phenomena are recurrent.
  5. The intensity of the EM radiation and the length of the ejection are correlated.
  6. The intensities of the phenomena are related to the intensity and the complexity of the magnetic fields in their locations.
- Those similarities hint at the possibility of a unified mechanism for all these phenomena.

### B - 3

GENERALIZED ROCHE POTENTIAL FOR MISALIGNED BINARY SYSTEMS

N. Schiller and Y. Avni

Department of Nuclear Physics, Weizmann Institute of Science,  
Rehovot

We have generalized the Roche potential for binary systems with any value of the angle between the axis of orbital revolution and the axis of rotation of the primary (and with zero eccentricity

orbit). Under the assumption of instantaneous hydrostatic equilibrium we have proved that the volume of the primary does not change with orbital phase to first order. Thus to avoid excessive mass transfer rates in x-ray binaries, the primary can fill its critical lobe only at the vicinity of those orbital phases where the critical volume has a minimum. We find that this occurs only at two orbital phases, corresponding to the passage of the secondary through the equatorial plane of the primary. We have discovered a new phenomenon: as the angle, between the rotation axis of the primary and the projection of the revolution axis onto the plane defined by the rotation axis and the line of centers, changes, outer and inner Lagrangian points may reverse their roles. A method for finding the truly inner Lagrangian point was developed, and the properties of the critical lobes were derived.

### B - 4

#### THE CENTRAL STAR EVOLUTION.

Amos Harpaz

Department of Physics and Astronomy, Tel Aviv University.

The evolution of a central star of a planetary nebula (CPN) is represented.

The question whether the Harman-Seaton sequence is an evolution path of a CPN or a locus of points representing different types of stars may be answered only by calculating a realistic evolution path of such a star. This evolution path is very sensitive to the initial model. Hence, arbitrarily chosen initial models lead to different paths in the H-R diagram. The results given here are of evolutionary calculations from an initial model which was obtained by continuous evolution along the asymptotic branch, and hence is supposed to be realistic.

The results are that along this path there is no increase of the luminosity coupled to the contraction of the star and the rising of the effective temperature - which means that the leftward moving of the star in the H-R diagram is on a horizontal line, and if this is the typical path of a central star, then the first part of the Harman-Seaton sequence, the upward moving line is a locus of points. It is reasonable that the descending part of the line is an evolution path.

The contraction until the effective temperature rises to  $40000^{\circ}\text{k}$  lasts for about 3000 years. In more 5000 years  $T_e$  continues to rise while the luminosity decreases slowly. In more a couple of thousands of years the luminosity drops faster,  $T_e$  begins to decrease and the star completes its loop-in the diagram-to the evolution path of a white dwarf.

B - 5PHYSICAL CONDITIONS IN AN OPTICALLY THIN GAS CLOUD IRRADIATED BY  $\gamma$ -RAYS

I. Kovner and M. Milgrom  
 Department of Nuclear Physics, Weizmann Institute of Science,  
 Rehovot

The positron density and the temperature are calculated in a relativistic plasma cloud ( $kT \gg mc^2$ ) irradiated by a plane-parallel flux of  $\gamma$ -rays with  $h\nu \gg mc^2$  assuming, that the cloud is optically thin for this  $\gamma$ -ray radiation.

In the extreme case of large  $\gamma$ -ray flux (for given spectrum) the temperature  $T$  approaches some constant value

$$T_{\max} \sim \left( \frac{mc^2}{k} \right) \cdot \left( \frac{h\nu}{mc^2} \right)^{1/3}, \text{ where } h\nu \text{ is a characteristic photon}$$

energy of the incoming radiation,  $m$  - electron mass.

The problem is relevant to the physics of  $\gamma$ -ray sources.

B - 6 INVITED

## OBSERVATIONAL EVIDENCES FOR NEUTRON STARS AND BLACK HOLES

J. Shaham, The Hebrew University, Jerusalem

B - 7

## THE GENERALIZATION OF THE MASS OPERATOR TO RIEMANNIAN SPACE-TIMES

Kh. Huleihil and S. Malin  
 Department of Physics, Ben-Gurion University of the Negev, Beer-Sheva

The generalization of the mass operator to Riemannian space-times is done by two approaches. The first is the analytic one. In this case there are three methods of generalization:

(a) Direct generalization of ordinary derivative to covariant derivative,  $\partial_\mu \rightarrow \nabla_\mu$ ; this generalization is the simplest one.

(b) The generalization which is invariant under the conformal transformations when  $m=0$ .

(c) The generalization of the product  $P_\mu P^\mu$  including determination of the order of the operators.

The second approach, which we call algebraic, is based on group theory. This approach can be applied only to some special cases. We discuss the de-Sitter model and a general Robertson-Walker space-time. In the Robertson-Walker space-time there is an operator suggested by Meggs. A criterion for choosing between the different possibilities is proposed. It is used to eliminate the Meggs operator, but is not stringent enough for a unique choice.

B - 8

## ISOTROPIC ANISOTROPY, GROUP OF MOTION AND DIMENSIONALITY OF SPACETIME

Elhanan Leibowitz

Department of Mathematics and Department of Physics,  
Ben-Gurion University of the Negev, Beersheva, Israel

Anisotropy in a Riemannian manifold, represented by a field of unit vectors, is not necessarily incompatible with the intuitive principle of "all directions are equivalent". To satisfy the fundamental "physical" postulate of isotropy, it is enough that the vector field exhibits rotational symmetry around itself. This condition can locally be cast into a covariant set of partial differential equations, its exact form being dependent on whether the dimensionality of the manifold is equal to or higher than three. The existence of an isotropic anisotropy restricts the metric of the manifold, again distinguishing the case of three dimensions. A relation is established between the isotropic anisotropies and the motions admitted by the manifold. The concepts discussed in this communication are applicable in relativistic cosmological models.

B - 9

## THE ACCELERATED SYSTEM WITH EUCLIDEAN SPATIAL GEOMETRY

Itzhack Dana

Technion-Israel Institute of Technology, Haifa, Israel.

We reconsider the transformation from an inertial system  $I$  to a noninertial one  $R$ , characterized by a Euclidean spatial geometry and accelerating in the direction of the  $X$ -axis of  $I$ .<sup>1,2</sup> Particular attention is given to the equation satisfied by the velocity of the points of reference of  $R$ , relative to  $I$ .<sup>3</sup> It is shown that the general solution of this equation displays a retarded (or advanced) character. This is interpreted in terms of the phase velocities of De-Broglie waves associated to a co-moving frame of reference representing  $R$ . The same point of view is adopted to find a class of space-time transformations to non-rigid frames  $R$ , which is invariant under Lorentz transformations  $I \rightarrow I'$ .

References:

1. C. Moller, The Theory of Relativity (Clarendon Press, Oxford, 1972).
2. E.T. Newman and A.I. Janis, Phys. Rev. 116, 1610 (1959).
3. G. Cavalleri and G. Spinelli, Nuovo Cimento 66B, 11 (1970).

WEDNESDAY AFTERNOON ,APRIL 9, 1980  
14:30

FEINBERG A

## C. METALS AND CONDUCTIVITY

N. Wisner - Bar Ilan Univ. - Presiding

### C-1 INVITED

ELECTRONIC PROPERTIES OF PURE AND DOPED POLYACETYLENE  
E. Ehrenfreund, Israel Institute of Technology, Haifa

### C-2

#### ELECTRICAL CONDUCTION IN DOPED POLYMERS

M. Shapira, Y. Schlesinger, V. Halpern and S. Baumel  
Department of Physics, Bar-Ilan University, Ramat-Gan

The effect of doping on the electrical properties of polymers such as polystyrene and polyparaphenylene has been studied. It is found that the introduction of suitable dopants increases the electrical conductivity of these materials by several orders of magnitude.

### C-3

#### RELAXATION TIME FOR ELECTRON-DISLOCATION SCATTERING\*

A. Bergmann, M. Kaveh and N. Wisner  
Department of Physics, Bar-Ilan University, Ramat-Gan

The angular dependence of the relaxation time appropriate for electron-dislocation scattering,  $\tau_{dis}(K)$ , has been calculated for polyvalent and noble metals. It is found that the importance of small-angle electron-dislocation scattering events leads to a marked  $K$ -dependence for  $\tau_{dis}(K)$ , where  $K$  denotes the point on the Fermi surface. For the spherical portions of the Fermi surface (the "bellies" of the noble metals),  $\tau_{dis}(K)$  is almost independent of  $K$ , whereas for the non-spherical portions of the Fermi surface (the "necks"),  $\tau_{dis}(K)$  is reduced by 1-2 orders of magnitude and thus essentially vanishes. The vanishing of  $\tau_{dis}(K)$  on the necks of the Fermi surface implies that the neck electrons are rapidly returned to thermal equilibrium and thus do not contribute to the resistivity. The above description applies to samples for which electron-dislocation scattering dominates the residual resistivity. However, for samples for which the residual resistivity arises primarily from electron-impurity scattering, the relaxation time is virtually independent of  $K$ . For such impurity-scattering dominated samples, it is just the neck electrons that are most

important for the low-temperature, electron-phonon scattering contribution to the resistivity  $\rho_{ep}(T)$ . Thus, the presence of a significant amount of electron-dislocation scattering will profoundly affect  $\rho_{ep}(T)$  at low temperatures by eliminating the contribution of the neck electrons. As a result,  $\rho_{ep}(T)$  will be significantly decreased by electron-dislocation scattering. These results are used to explain recently reported anomalies for the low-temperature electrical resistivity of Ag and Al. Finally, it is explained why the present results apply only to the polyvalent and noble metals, but not to the alkali metals.

\* Supported in part by the Israel Commission for Basic Research.

### C - 4

#### MEASUREMENT OF SHAPIRO-STEPS IN GRANULAR ALUMINUM MICROBRIDGES

B. Dvir and G. Deutscher

Dept. of Physics and Astronomy, Tel-Aviv University, Israel

Josephson microbridges find numerous applications as SQUIDS, detectors, computer elements etc.. Granular materials, especially aluminum and lead, are most suitable for making such bridges, because of their low critical current and high critical temperatures. Since granular Al bridges have been used successfully in RF SQUIDS<sup>1</sup> although their dimensions are much larger than the coherence length (typically  $< 100 \text{ \AA}$ ), it was desirable to investigate the existence of microwave-induced steps in those bridges.

Microbridges of dimensions  $2.5 \times 7.5 \text{ \mu m}$  (WxL) have been fabricated on  $1000 \text{ \mu m-cm}$  Al-Al<sub>2</sub>O<sub>3</sub> thin ( $1000 \text{ \AA}$ ) films by using projection lithography and etching techniques. The resulting bridges had critical currents of  $15 \text{ \mu A}$  and  $T_c = 2.2 \text{ K}$ .

Their I-V characteristics were studied at different temperatures with low-noise measurement equipment ( $V_n < 0.2 \text{ \mu V rms}$ ) under microwave irradiation at 10 and 30 GHz. In those bridges no steps have been detected, and the only effect of the radiation was shifting of the I-V curves towards lower critical currents, probably because of heating.

Smaller microbridges -  $0.6 \times 1.2 \text{ \mu m}$ , and variable-thickness bridges (VTB) have been fabricated, using similar techniques. The VTB were made of dual-layer material: pure Al on top of the granular material. The microbridge itself was thinner and composed only of the granular aluminum, with pure Al banks.

---

1 ref: D. Abraham et al., in Jour. of Low Temp. Phys., 32, 853 (78)

C - 5

## CHARGED BOSONS IN A RANDOM POTENTIAL

M. Ya. Azbel  
 Department of Physics and Astronomy, Tel Aviv University,  
 Ramat Aviv, Israel

It is shown that the interaction of bosons in a random potential in certain cases provides extended states. Extended or localized states of interacting bosons in a random potential, as well as their Bose-condensation, depend on the statistics and the form of potential wells, and therefore, e.g., on the pressure.

C - 6

## THE PHONON-DRAG CONTRIBUTION TO THE ELECTRICAL RESISTIVITY OF POLYVALENT METALS: ALUMINUM\*

M. Brody, M. Kaveh and N. Wisner  
 Department of Physics, Bar-Ilan University, Ramat-Gan

The theory of the phonon-drag contribution  $\rho_g(T)$  to the electrical resistivity of polyvalent metals is developed, taking explicit account of the multiple-plane-wave character of the pseudo-wave function. Use of a multiple-plane-wave pseudo-wave function profoundly affects all aspects of the calculation of  $\rho_g(T)$ , including (i) the electron distribution function, (ii) the Fermi surface, (iii) the electron velocities, and (iv) the electron-phonon scattering probability. The coupled electron and phonon Boltzmann equations are solved to obtain the phonon distribution function  $\phi_{ph}$  in terms of the electron distribution function  $\phi_{e1}$ . It is shown that for any polyvalent metal,  $\rho_g(T)$  is negligible throughout the low-temperature regime ( $T \lesssim 10^2$  K), because of important cancellation effects that occur only for polyvalent metals. These qualitative results for  $\rho_g(T)$  are fully confirmed quantitatively by an explicit calculation for Al, a typical polyvalent metal. The result that  $\rho_g(T)$  is negligible for polyvalent metals is in marked contrast to the result for the alkali metals, for which these cancellation effects do not occur and consequently  $\rho_g(T)$  is very large at low temperatures. The Ziman approximation to  $\phi_{ph}$  and  $\rho_g(T)$  is also analyzed and found to be seriously in error. In particular, according to the Ziman approximation,  $\rho_g(T)$  is not negligible at low temperatures and leads to a measurable reduction, of order 10%, of the resistivity of Al above about 5 K. Finally, a discussion is given of previous work, in which it is shown that the previous calculation of  $\rho_g(T)$  for Al is incorrect.

\*Supported in part by the Israel Commission for Basic Research.

C - 7 INVITED

## CONDUCTIVITY IN CHARGE-DENSITY-WAVE SYSTEMS

B. Horovitz, The Weizmann Institute, Rehovot

C - 8

## QUENCHING OF PHONON-DRAG RESISTIVITY IN POTASSIUM\*

M. Danino, M. Kaveh and N. Wiser

Department of Physics, Bar-Ilan University, Ramat-Gan

Recent ultra-high-resolution measurements<sup>1-3</sup> of the low-temperature electrical resistivity of potassium have revealed an unexpected sample dependence for the electron-phonon scattering term  $\rho_{ep}(T)$ . A comparison of all the available data<sup>1-3</sup> for potassium shows that the variation of  $\rho_{ep}(T)$  from sample to sample increases markedly with decreasing temperature, going from about 25% at 4 K, to about 50% at 3 K, and to nearly a factor of 3 at 2 K. Our explanation for these results is based on the idea that electron-dislocation scattering quenches the phonon-drag contribution  $\rho_g(T)$  to  $\rho_{ep}(T)$ . The presence of a large negative  $\rho_g(T)$  requires that the electron distribution function be characterized by an isotropic relaxation time. If the residual resistivity of a sample is dominated by electron-impurity scattering, then the electron relaxation time will indeed be isotropic and the full phonon-drag term  $\rho_g(T)$  will be present, resulting in a greatly reduced value for  $\rho_{ep}(T)$ . However, if the residual resistivity of a sample is dominated by electron-dislocation scattering, then the relaxation time will be anisotropic over the Fermi surface,  $\rho_g(T)$  will be quenched, and the resulting  $\rho_{ep}(T)$  will be much larger. For the intermediate case, for which comparable amounts of electron-impurity scattering and electron-dislocation scattering are present,  $\rho_g(T)$  will be partially quenched. Thus, for any particular sample, the value obtained for  $\rho_{ep}(T)$  will depend on the extent to which  $\rho_g(T)$  is quenched, which in turn depends on the relative proportions of electron-impurity scattering and electron-dislocation scattering. These ideas have been developed into a quantitative theory of the sample dependence of  $\rho_{ep}(T)$ . The theoretical results are in excellent agreement with all the recent data<sup>1-3</sup> for potassium.

\* Supported in part by the Israel Commission for Basic Research.

<sup>1</sup>H. van Kempen et al., Phys. Rev. Lett. 37, 1574 (1976).

<sup>2</sup>J.A. Rowlands et al., Phys. Rev. Lett. 40, 1201 (1978).

<sup>3</sup>B. Levy, M. Sinvani and A.J. Greenfield, Phys. Rev. Lett. 43, 1822 (1979).



C - 9

## QUANTUM PARTICLE IN 1-D POTENTIALS WITH INCOMMENSURATE PERIODS

M. Ya. Azbel

Dept. of Physics and Astronomy, Tel Aviv University, Ramat Aviv,  
Tel Aviv, Israel

The energy spectrum and wave functions for a particle in periodic potentials with incommensurate periods are obtained analytically and reduced to specific phase trajectories. The spectrum is of the devil's stairs type. States may be extended and localized, separated by mobility edges. These results are applicable to incommensurate linear chain structures (such as those in  $\text{Hg}_{3-\delta}\text{AsF}_6$ ) and to the fine structure of de Haas-van Alphen oscillations.

C - 10

## THE NATURE OF THE CONTINUOUS TIME RANDOM WALK APPROXIMATION

V. Halpern

Department of Physics, Bar-Ilan University, Ramat-Gan, Israel

## Abstract

The standard continuous time random walk approximation for the electrical conductivity of amorphous solids is derived from the rate equations appropriate to non-interacting electrons in localised states. This derivation suggests an improved method of averaging the waiting-time distribution, and also shows that the CTRW is equivalent to the virtual crystal approximation used for alloys. Some consequences of this equivalence are discussed.

C - 11

## EFFECT OF ANNEALING ON THE TEMPERATURE DEPENDENCE OF THE ELECTRICAL RESISTIVITY OF ALUMINUM\*

M. Sinvani and A.J. Greenfield

Department of Physics, Bar-Ilan University, Ramat-Gan

The temperature-dependent part  $\rho(T)$  of the electrical resistivity of Al has been measured from 1.3-4.2 K, using an apparatus capable of achieving 2 ppm relative accuracy. The measurements were carried out for a series of samples which had been successively annealed at progressively higher temperatures. The most interesting feature of the data is that  $\rho(T)$  varied from sample to sample in a systematic way as a result of the annealing process. Since the effect of annealing is primarily to reduce the dislocation

density in the sample, we associate the sample dependence of  $\rho(T)$  with the varying density of dislocation lines present in the various samples. To understand these results, one writes  $\rho(T) = \rho_{ee}(T) + \rho_{ep}(T)$ , in terms of the electron-electron scattering contribution and the electron-phonon scattering contribution, respectively. The data show that  $\rho_{ee}(T)$  decreases upon annealing, whereas  $\rho_{ep}(T)$  increases upon annealing. These results are shown to be in agreement with the prediction of recent theoretical work.

\*Supported in part by the Israel Commission for Basic Research

### C - 12

#### MICROWAVE PROPAGATION IN SIMPLE METALS AND FERMI-LIQUID EFFECTS

I.D. Vagner

Department of Physics, Technion, Haifa, Israel

In the framework of the theory of the gyrorelaxation damping of a helicon wave [1] the dependence of the microwave damping on the Fermi-liquid parameters was considered. The physical origin of this effect can be understood as follows: the adiabatical invariance of the magnetic moment  $\vec{M}$  of the rotating electron:  $\vec{M} = \vec{l} \cdot \vec{s} = \mathcal{E}_f/B$  leads to the periodic variation of the quasi-particles transverse distribution. The electron-electron scattering tries to equalize the quasiparticle distribution in the transverse and longitudinal directions to the external magnetic field. As a result there exists an energy transfer from the varying time-dependent magnetic field to the electron subsystem, which results in the damping of the microwave under such conditions.

1. I. Vagner, Phys. Lett. 62A, 149, 1977.

C - 13

## EXACTLY SOLVABLE MICROSCOPIC GEOMETRIES AND RIGOROUS BOUNDS FOR THE COMPLEX DIELECTRIC CONSTANT OF A TWO-COMPONENT COMPOSITE MATERIAL

D.J. Bergman

Department of Physics and Astronomy, Tel Aviv University,  
Ramat Aviv, Israel

P. Lacour-Gayet

Schlumberger-Doll Research, Ridgefield, Connecticut 06877, U.S.A.

Exact bounds for the complex bulk effective dielectric constant  $\epsilon_e$  of a two-component macroscopic composite that depend on the available information about the composite are presented and discussed. The bounds have a very simple geometrical representation and construction as allowed regions in the complex  $\epsilon_e$ -plane. The extreme limits of the various allowed regions are attainable in all cases by special, exactly solvable microscopic geometries. As a consequence, it is shown that there can exist composites where the real part of  $\epsilon_e$  diverges as  $\omega \rightarrow 0$  while the d.c. conductivity  $\sigma_e \neq 0$ .

WEDNESDAY AFTERNOON, 9 APRIL, 1980

FEINBERG B

14:30

**D. OPTICS AND LASERS**

**I. Smilanski - Nuclear Research  
Center, Negev, Beer Sheva - Presiding**

**D-1 INVITED****LASER RESONATORS WITH PHASE-CONJUGATE MIRRORS**

**A. Hardy, Weizmann Institute of Science, Rehovot**

**D-2****INFRA-RED OPTICAL FIBERS**

**R. Arieli, A. Katzir  
Department of Physics and Astronomy, Tel Aviv University  
Ramat Aviv, Israel**

In this work we have tried to fabricate an optical fiber that will be transparent in the middle infrared ( $\lambda = 3-30 \mu\text{m}$ ). The glass fibers which are in use in optical communication are transparent for wavelengths  $\lambda < 3 \mu\text{m}$ , and they may have losses as low as 0.5 dB/Km. It has been suggested that ideal fibers, transparent in the middle infrared, will have losses in the order of  $10^{-4}$ - $10^{-5}$  dB/Km. Fibers with such incredibly low losses may have several applications. First, they may be used in long-distance optical communication. Second, they may be used in conjunction with infrared detectors for detection and for thermal imaging. And last, but not least, they may find uses in power transmission; it is expected that tens of watts of energy of  $\text{CO}_2$  laser radiation will be transmitted through these low loss fibers, and may be used in endoscopic laser surgery or in industrial processes.

In our research we have chosen inorganic crystals as our starting material, because of their transparency in the infrared, and we fabricated  $\text{AgCl}$  fibers by extrusion in the 25 - 200°C temperature range. Several meters of such fibers were tested for transmission, using a continuous  $\text{CO}_2$  laser ( $\lambda = 10.6 \mu\text{m}$ ) and He-Ne laser ( $\lambda = 0.6 \mu\text{m}$ ). The transmission was found to be about 5% per meter at both wavelengths. The fibers were very flexible, and they did not lose their flexibility even at liquid nitrogen temperature ( $T = 77^\circ\text{K}$ ).

D-3WAVELENGTH-TIME MULTIPLEXING FOR DIRECT PICTURE TRANSMISSION  
IN SINGLE OPTICAL FIBERS

U. Levy and A.A. Friesem,  
Dept. of Electronics, Weizmann Inst. of Science, Rehovot, Israel

Direct picture transmission in a single step-index optical fiber by angular time multiplexing or by angular wavelength multiplexing were demonstrated<sup>1,2</sup>. We have recently extended these investigations to include direct transmission by multiplexing the information in the remaining combination of coordinates, namely time and wavelength. Unlike the multiplexing techniques that involve the angular coordinate, the quality of the picture in the wavelength-time multiplexing scheme, essentially does not degrade with length. Thus it is now possible to transmit pictures of 100 x 100 resolution elements through single fibers 500 meters long. The details of the multiplexing scheme and its limitations will be described and supporting experimental results will be presented.

1. U. Levy and A.A. Friesem, Appl. Phys. Lett. 32, 29 (1978).
2. A.A. Friesem and U. Levy, Optics Letters, 2, 133 (1978).

D-4OPTICAL PROPERTIES OF A BEAM REFLECTED THROUGH A TURBULENT  
ATMOSPHERE\*

D. Bensimon, A. Englander, S. Shtrikman, M. Slatkine and D. Treves  
Dept. of Electronics, Weizmann Inst. of Science, Rehovot, Israel

Optical beams retroreflected through a turbulent atmosphere have been considered in recent years mainly in conjunction with pollution monitoring and laser radars (LIDAR). We have recently made use of a retroreflected HeNe laser-beam to conveniently measure the atmospheric structure constant  $C_n^2$  over an unsaturated optical path of 0.5 km length [1]. We have also measured the optical properties of the reflected waves by using both direct and heterodyne detection techniques [1]. In the following we present an extension of the optical measurements up to 6 km path lengths (12km total path). The measuring system has been modified to include at one end of the path a 15 mW He-Ne laser transmitter (diffraction limited 1 cm aperture) separated from the receiving optics (5 cm aperture). This was done to prevent interference between backscattered radiation from the transmitting optical components and the beam reflected through the turbulent atmosphere. At the other end of the path we have placed a 5 cm diameter glass corner cube. The reflected beam was either directly detected by a low noise fast Si avalanche photodiode, or combined with a frequency shifted (40 MHz) local oscillator for heterodyne detection. The frequency shift was generated acoustooptically. We

present results of measurements of scintillation histograms, scintillation time correlation and power spectra and angle of arrival of the beam. We find that the Log-Normal intensity distribution holds also for the 12 km double path although the standard deviation  $\sigma$  was  $\sim 2$  [2]. Similarly the intensity power spectrum obeys the  $f^{-8/3}$  law. The wave amplitude and phase statistics, measured through the heterodyne scheme, differ slightly from Log-Normal. A discussion of these will be presented. Finally we shall describe the use of angle of arrival measurements and coherence length  $\rho_0$  [2] to determine the atmospheric structure constant  $C_n^2$  over long turbulent paths. Comparison with  $C_n^2$  determination over short paths by use of scintillation statistics will also be given.

(\*) Work supported by a grant of the National Council for Research and Development in Israel.

[1] D. Bensimon, A. Englander, S. Shtrikman, M. Slatkine, D. Treves, Proceedings of the 11th Convention of IEEE in Israel, paper C3-4, Oct. 1979.

[2] R.L. Fante, Proceedings of the IEEE 63, 1669 (1975).

D-5

**TESTING OF ASPHERICAL SURFACES\***

Joshua Gur

Jerusalem College of Technology, Jerusalem, Israel

*Testing of aspherical surfaces is extremely important in their production process. Most of the appropriate methods were investigated. A critical review is presented. The ronchi test is found to be simple, inexpensive reliable, and accurate enough for a broad range of applications. The ronchi fringes are displayed on a C.R.T. and compared with the ideal fringes computed by a microprocessor.*

\* This work was done while the author was in RAFAEL.

D - 6

## REAL-TIME HOLOGRAPHIC DEFORMATION MEASUREMENTS

A.A. Friesem, Y. Katzir and B. Sharon

Dept. of Electronics, Weizmann Inst. of Science, Rehovot, Israel

Techniques for accurate, non contacting quantitative measurements of deformations in opaque, diffuse objects are described. These involve a combination of real-time holographic interferometry with digital, automatic data acquisition and reduction. Holographic interferograms, obtained with the aid of photoconductor-thermo-plastic devices, are electronically scanned with a linear photodiode array, and the data is acquired at a rate of 70  $\mu\text{sec}/\text{point}$  by a microcomputer. The data is then transmitted to a large computer for processing, and the results are displayed on a graphics terminal. A single image is so processed to yield the deformation function for about 100 object points, with an r.m.s. error of  $\lambda/80$ . These techniques were tested in the laboratory for detecting flaws in industrial parts, and the results are presented.

D - 7SUBMICRON PERIODIC CORRUGATIONS FABRICATED BY CHEMICAL ETCHING IN  $\text{Pb}_{1-x}\text{Sn}_x\text{Te}$ 

E. Kapon and A. Katzir

Department of Physics and Astronomy, Tel Aviv University, Ramat Aviv.

Periodic corrugations, suitable for use in distributed feedback injection lasers, were fabricated on  $\text{Pb}_{1-x}\text{Sn}_x\text{Te}$  substrates using chemical etching. A thin film of photoresist (Shipley AZ-1350B) was spin coated on a polished  $\text{Pb}_{1-x}\text{Sn}_x\text{Te}$  substrate, and exposed to the interference pattern formed by splitting and then recombining a HeCd ( $\lambda=0.4416\mu\text{m}$ ) laser beam. Development (Az-developer) resulted in a photoresist mask in the form of a relief grating. This relief pattern was transferred to the substrate by etching with 1%  $\text{Br}_2$  in HBr through the resist mask. Slightly over-exposed photoresist gratings were used to allow the etchant to reach the substrate. The corrugations thus achieved were 0.25  $\mu\text{m}$  deep; the period, chosen to provide distributed feedback in first Bragg order for a typical  $\text{Pb}_{1-x}\text{Sn}_x\text{Te}$  diode laser, was 0.75  $\mu\text{m}$ .

The grating depth required for distributed feedback operation was calculated for various tooth shapes. For a typical  $\text{Pb}_{1-x}\text{Sn}_x\text{Te}$  laser 750  $\mu\text{m}$  long, the depth was found to be 1600 $\text{\AA}$ , 2000 $\text{\AA}$ , and 2400 $\text{\AA}$  for rectangular, sinusoidal and symmetric triangular grating, respectively. This is within the capability of the fabrication method described above.

D - 8

## TRANSVERSE-MODE MATCHING IN UNSTABLE-RESONATOR INJECTION-LOCKING

Y. Kedmi and D. Treves  
Dept. of Electronics, Weizmann Inst. of Science, Rehovot, Israel

Laser injection locking is a method for controlling the wavelength and linewidth of a high power laser by injection of a low power signal into it. In order to have efficient locking of the laser line on the injected signal it is important to obtain maximum coupling between the signal and the laser mode. The problem of transverse-mode matching between a Gaussian beam and the lowest-loss mode of an unstable resonator into which this beam is injected is considered. The beam is injected through a small coupling hole in the center of the resonator back-mirror. The resonator modes are numerically computed along with the distribution of the injected signal inside the resonator, and the coupling coefficient between them is calculated. The computations are carried out for various diameters of the coupling hole, and for different Fresnel numbers.

D - 9

## KINETIC INVESTIGATION OF THE UPPER LASER LEVELS OF THE COPPER VAPOR LASER LINES

J. Tenenbaum, I. Smilanski and S. Lavi  
Nuclear Research Centre-Negev, Beer Sheva, Israel

A Modernized hook apparatus was used to study the population history of the  $P_{3/2}$  and  $P_{1/2}$  upper laser levels of the copper vapor laser. A detailed description of the method and apparatus was given elsewhere <sup>(1)</sup>. We studied the dependence of the level populations on the input power. The  $P_{3/2}$  level was studied using the doublet 5218 and 5220 nm;  $4p^2P_{3/2} - 4d^2D_{5/2}$  and  $4p^2P_{3/2} - 4d^2D_{3/2}$  transitions while the  $P_{1/2}$  level was studied using the 5153 nm;  $4p^2P_{1/2} - 4d^2D_{3/2}$  transition.

The results indicate three dominant features: (1) The level population rate depends weakly on the input power. (2) The lifetimes of both levels are the same for the same experimental conditions and are inversly proportional to the input voltage. This emphasises the role of the discharge on the deexcitation of those levels. (3) The maximum populations of both levels become saturated beyond some critical input power.

1. I. Smilanski et al, Optics Letters, March 1980.



D - 10

## PREIONIZATION EFFECT ON A COPPER VAPOR LASER

S. Gabay and I. Smilanski  
Nuclear Research Centre-Negev, Beer Sheva.

There is a large scatter in the appropriate E/p values for the operation of a copper vapor laser. Carefull examination of the experimental conditions indicates that the scatter in these values is according to the number of electrons which remain in the gas prior to the excitation pulse. Preionization improves the discharge conditions and reduces the required E/p value. We found a clear evidence of the preionization influence by operating the laser in the burst mode. In this mode, and for a low E/p, the first pulse in each burst does not induce lasing. The laser output increases in the following pulses and levels off after few pulses. By reducing the buffer gas pressure, the steady state is achieved closer to the beginning of the burst.

In order to examine the preionization influence, we introduced a separate preionization electrode into a copper vapor laser heated by an external oven. At buffer gas pressure of few torrs a dramatic increase in the laser output was observed at 1  $\mu$ sec time separation between the excitation pulse and the preionization pulse. As the buffer gas pressure was increased to a value of more than 50 torr, the laser output was found to be a function of the delay between the excitation and the preionization pulses. The time constant of this function was similar to the free electron diffusion time constant.

D - 11

## INVESTIGATION OF LONGITUDINAL PUMPING OF DYE LASERS BY A COPPER VAPOR LASER

M. Amit, S. Lavi, E. Miron and G. Erez  
Nuclear Research Centre-Negev, Beer-Sheva

A narrowband, tunable, powerful and high repetition rate laser is an extremely useful laboratory tool. A copper vapor laser (CVL) pumped dye laser seems a good choice for such a purpose. We use an unstable resonator copper vapor laser with average output power of 10 watts (4 kHz rep. rate) at two spectral lines: green (511 nm; 6 watts) and yellow (578 nm; 4 watts).

Basically there are two modes of pumping; transverse - where the CVL beam is perpendicular to the dye laser axis, and longitudinal where the pump is approximately colinear with the dye laser axis. The transverse pumping mode has been extensively investigated, while the longitudinal pumping configuration has not been sufficiently tested. We present results of experiments which have been aimed to determine optimum operation parameters of longitudinally pumped dye laser. This study is necessary for the choice between the two pumping modes.

A few longitudinal and almost longitudinal configurations have been tested and optimized. The effects of the dye cell, dye concentration and output coupler on the conversion efficiency were tested for each configuration. A wideband laser could be operated with an efficiency of about 40%. The use of a grating in Littrow configuration and introduction of a telescope into the cavity narrowed the bandwidth to 0.02 nm but the efficiency reduced to 8%. The use of the same cavity components with transverse pumping resulted in a similar bandwidth but at efficiency of about 25%. Another disadvantage of longitudinal pumping (when compared to transversal) is that only the green line can be used for pumping Rhodamine B. The use of the yellow line results in unfavorable yellow stimulated emission which reduces the output power of the dye laser.

D - 12

## OPTICAL SECOND HARMONIC GENERATION IN COLLAGEN\*

S. Roth and I. Freund  
Department of Physics, Bar-Ilan University, Ramat-Gan

Structural properties of ordered collagen in native, rat tail tendon have been studied by means of optical second harmonic generation. Polarization and angular divergence measurements were made from tendons kept in natural physiological buffer. Two independent hyperpolarizability tensor elements,  $\beta_{31}$  and  $\beta_{33}$ , of about the same magnitude have been found, in accordance with the fibril  $C_{\infty}$  symmetry. The angular scattering consists of a forward, sharp, less than 1.5 mrad peak, and a much lower background. The peak reveals the existence of coherent order across the whole tendon and taking into account the polar  $\beta_{31}$  and  $\beta_{33}$  elements, the tendon is established to be polar.

\*Supported in part by the Israel Commission for Basic Research.

D - 13

## RELATIVE TWO-PHOTON ABSORPTION MEASUREMENTS IN THE UV

Haim Lotem\*, N.R.C.N. P.O. Box 9001, Beer-Sheva Israel.  
 Cid B. de Araujo, Department of Physics, Universidade Federal  
 Pernambuco, 50000 - Recife - Brasil.

The study of Two-Photon Absorption (TPA) of solids in the UV attracts increasing scientific and technological interest due to the wide spread and growing use of high power UV lasers. The TPA coefficients of 5 alkali-halides crystals at  $2\hbar\omega=7.12\text{eV}$  ( $\omega$  is the second harmonic of a Ruby laser) at room temperature, are reported here. The measurements were performed using a 20 nsec pulsed Ruby laser efficiently doubled in a CDA phase-matched crystal. The nonlinear absorption versus the laser intensity is compared with that of a reference RbI crystal. The relative TPA results are as follow:-

RbI (1.); RbBr ( $0.49 \pm 0.17$ ); KBr ( $0.71 \pm 0.21$ );  
 KI ( $1.02 \pm 0.30$ ) and KCl ( $< 0.05$ ).

No attempt was made to obtain absolute cross sections because the temporal and spatial laser parameters are not measurable. We note that a possible method for obtaining absolute TPA cross sections is by calibrating the TPA measurement versus the stimulated Raman (or Invers-Raman) effect using two laser frequencies.

Our results fit within a factor of two with other reported measurements in the nsec region at  $2\hbar\omega=6.7\text{eV}$ , (1) with psec measurements at  $2\hbar\omega=7\text{eV}$ , (2) and with earlier nsec works from the mid sixties.

\* This experimental work was performed at the Grodon McKay Laboratory, Harvard University, while the authors stayed there as Postdoctoral Fellows.

- (1) Yehiam Prior and Hans Vogt, Phys. Rev. B19 ,5388(1979).
- (2) P. Liu, W.L. Smith, H. Lotem, J.H. Bechtel, and N. Bloembergen, Phys. Rev. B17 , 4620 (1978).

D - 14

## INTENSITY FLUCTUATIONS OF A PLANE WAVE PROPAGATING IN AN ANISOTROPIC RANDOM MEDIUM

M. Tur and M.J. Beran  
 Faculty of Engineering, Tel-Aviv University, Tel-Aviv, Israel

Intensity fluctuations of a plane wave propagating in an anisotropic random medium is investigated for low frequency radiation using the parabolic approximation and perturbation techniques. Theoretical expressions are derived for the range dependence of the intensity fluctuations and their correlations. When  $k\ell_H \gg 1$  and  $k\ell_V^2/\ell_H$  ( $k$  is the radiation wave number,  $\ell_H$  and  $\ell_V$  are mutually perpendicular, horizontal and vertical characteristic correlation lengths of the medium), explicit results are given for horizontal propagation (parallel to  $\ell_H$ ). It is shown

that the fluctuation index  $\sigma_I^2$  is proportional to the range  $z$  and not to  $z^3$  as it is in isotropic media. Numerically, we also calculate the intensity fluctuations of a plane wave, whose propagation direction forms an arbitrary angle with the principal axes defined by  $l_V$  and  $l_H$ . We find that the magnitude of the fluctuations is very sensitive to the propagation angle. Two examples are discussed: an exponential correlation function which approximates the ocean temperature microstructure, and a Gaussian correlation function.

#### D - 15

##### NUMERICAL INVESTIGATIONS OF FINITE BEAM PROPAGATION IN ISOTROPIC RANDOM MEDIA

M. Tur and M.J. Beran

Faculty of Engineering, Tel-Aviv University, Tel-Aviv, Israel

The differential equation for the fourth order, statistical moment of the field of a finite beam, propagating in a statistically homogeneous and isotropic two-dimensional random medium is solved numerically. Results are presented for the variance and covariance of irradiance scintillations both on and off axis. It is shown that the range dependence of the variance is highly dependent on the ratio  $D/l_n$  ( $D$  - initial beam width,  $l_n$  - correlation length of a medium with a Gaussian correlation function and approaches that of a plane wave for large enough  $D/l_n$ . It is also found that the variance increases towards the edge of the beam in qualitative agreement with previous Rytov based theoretical predictions.

#### D - 16

##### LASER RESONATORS WHICH CONTAIN SATURABLE GAIN MEDIUM: A RAY-MATRIX APPROACH

A. Hardy

Dept. of Electronics, Weizmann Inst. of Science, Rehovot, Israel

Laser cavities which contain saturable gain medium are analyzed by applying ray-matrix techniques. The finite end mirrors are approximated by mirrors having gaussian reflectivity profile. A self-consistent equation is derived which takes into account the effect of the medium on the beam's parameters, as well as the gain saturation by the circulating gaussian beam. The approach provides a useful analytical approximation to the mode calculation of practical laboratory lasers which operate well above threshold.

D - 17**A NOVEL BEAM QUALITY MEASUREMENT TECHNIQUE AND PARAMETERIC STUDY OF AN UNSTABLE RESONATOR COPPER VAPOR LASER**

S. Lavi, S. Gabay, E. Miron, G. Erez and I. Smilanski  
Nuclear Research Center Negev, P.O. Box 9001, Beer-Sheva

The traditional design of the copper vapor laser (CVL) consists of a flat - flat stable resonator and the typical beam divergence is about 200X diffraction limit. This quality is not satisfactory for some applications such as oscillator-amplifier staging and dye laser pumping. A significantly better beam divergence is achieved with an unstable resonator. We report the influence of resonator parameters such as magnification and Fresnel number on the beam divergence and the output power for a CVL operating at the positive branch of an unstable confocal resonator. The most striking result is the reduction of the beam divergence by a factor of 40 (to 0.15 mrad which is about 5X diffraction limit), while retaining the same output power.

Measurements of such small beam divergences are usually not straightforward. A simple and convenient method is to focus the beam by a long focal-length mirror, magnify the spot by a vidicon CCTV camera and to determine the spot size using a single line selector system(1). The precision of this method is limited by off-axis aberrations, calibration of the CCTV image magnification, and the dimensions of the laboratory. These limitations are overcome by replacement of the mirror with a high quality telescope and the use of a Fabry-Perot etalon. The etalon enables focus adjustment of the telescope and provides "in-situ" calibration. The interference fringe pattern produced by the measured CVL beam is used to calculate the relation between beam divergence and the spot size image. This general technique is suitable for beam divergence measurement of monochromatic beams and is capable of handling single pulses.

- (1) S. Lavi, E. Miron and I. Smilanski, "Spectral distribution measurement of single laser pulses", Opt. Comm. 27 117-120 (1978).

D - 18THEORY OF RESONANCES IN THE ELECTROMAGNETIC SCATTERING BY  
MACROSCOPIC BODIES\*

D.J. Bergman

Department of Physics and Astronomy, Tel Aviv University,  
Ramat Aviv, Israel

D. Stroud

Department of Physics, The Ohio State University,  
Columbus, Ohio 43210, U.S.A.

The electromagnetic scattering resonances of a collection of macroscopic bodies with uniform electric properties are used to construct a spectral representation for the scattered field. The resonances and their weights are found by solving for the eigenvalues and eigenstates of a non-hermitian, linear integral operator  $\Gamma$ . A scheme is developed for doing this by diagonalizing a matrix that represents  $\Gamma$  by the set of individual grain eigenstates - the diagonal elements are individual grain eigenvalues while the off-diagonal elements are overlap integrals of eigenstates from two different grains. For a system of spherical scatterers, this leads to a reasonable method of calculating numerically the scattered field in cases where the multiple scattering is important. As an example, the scattering by a pair of identical spheres is worked out analytically for a limiting case. Sum rules for the weights in the spectral representation are derived and discussed.

\* Research supported in part by the United States - Israel Binational Science Foundation under Grant No. 2006/79.

WEDNESDAY AFTERNOON, APRIL 9, 1980  
14:30

FEINBERG D

## E. PLASMA PHYSICS I.

B.S. Frenkel - Hebrew University, Jerusalem - Presiding

### E-1 INVITED

INTERACTION OF INTENSE PARTICLE BEAMS WITH MATTER

Z. Zinamon, The Weizmann Institute, Rehovot

### E-2

NON-IDEAL EFFECTS ON THE STABILITY OF A CYLINDRICAL CURRENT-CARRYING PLASMA

L. Gomberoff  
Department of Physics and Astronomy, Tel Aviv University,  
Ramat Aviv, Israel

The stability of a cylindrical plasma, limited by fixed boundaries, is considered. For parallel wave number  $k_{\parallel} \approx 0$ , non-ideal effects are important. Solutions of the linearized equations including viscosity, thermal conductivity, and resistivity are obtained, and it is shown that a marginal mode with  $k_{\parallel} = 0$  exists when a critical pressure gradient is attained. This mode characterizes the onset of large-scale steady convection in the plasma.

### E-3

ON THE MAXIMUM THERMONUCLEAR YIELD IN ION BEAM - DT PELLETT FUSION

S. Cuperman and B. Levush  
Department of Physics and Astronomy, Tel Aviv University,  
Ramat Aviv, Israel

We have undertaken a systematic theoretical search for conditions providing maximum thermonuclear yields in ion beam-DT pellet systems. In this, the variable parameters were the initial ion beam power,  $P_0$ , the initial kinetic energy of the ions in the beam,  $E_i$ , and their atomic characteristics (mass and charge).

The pellet used in this work consists of a neutral plasma which comprises electrons and a 50-50% deuteron-triton mixture. Each of the electron and ion (having effective charge  $\bar{Z}$  and effective mass  $\bar{M}$ ) components is treated as an ideal gas subsystem having

distinct characteristics (e.g.,  $T_e \neq T_i$ , etc.); the streaming velocity is considered to be identical. The incident ion beam consists of a spherically symmetric flow of fast ions impinging on the pellet and has a laser-like time profile,  $P = P_0 \cdot (1 - t/t_0)^2$ . The monoenergetic beam-ions behave like "test" particles which interact with the pellet-plasma particles through Coulomb interactions.

Among other results, we have found that relatively large parameter ranges of initial beam power and kinetic energy for significant thermonuclear yields exist; maximum yields can be achieved by the proper selection of the parameter values. More details will be presented.

#### E - 4

#### THE ELECTROSTATIC INSTABILITY OF RIPPLED, MAGNETICALLY FOCUSED, NON-NEUTRAL, CYLINDRICAL BEAMS OF CHARGED PARTICLES

S. Cuperman and F. Petran  
Department of Physics and Astronomy, Tel Aviv University,  
Ramat Aviv, Israel

The stability of rippled non-neutral beams of charged particles produced under conditions in which centrifugal, space charge and magnetic forces close to the emitting cathode are not balanced, is investigated. The beams are considered to be cold and assumed to partly fill a conducting pipe in the presence of an axial uniform magnetic field. The calculations hold for long wavelength electrostatic perturbations (or, alternatively, thin beams) and small ripple amplitudes (i.e., close to the laminar regime).

The rippled equilibrium beams considered in this work are found to support unstable, azimuthally symmetric, electrostatic modes. The growth rates are proportional to the relative ripple amplitude and to the plasma frequency of the rippling particles.

The entire process can be viewed as a three-wave parametric interaction of stimulated Raman type in which a static pump (the periodic E-field corresponding to the rippled beam equilibrium) decays into two space charge waves of the partly filled cylindrical waveguide.



E - 5**ON THE PARAMETRIC DEPENDENCES OF THE BEAM-PLASMA-DISCHARGE AT LOW PRESSURES AND MAGNETIC FIELD STRENGTHS****S. Cuperman and I. Roth****Department of Physics and Astronomy, Tel Aviv University,  
Ramat Aviv, Israel****W. Bernstein****Department of Space Physics, Rice University, Houston, U.S.A.**

We present the results of the calculations we carried out in order to explain the relationship between the critical current and the physical parameters in the beam-plasma-discharge at low pressures and magnetic fields reported by Bernstein et al. [1980].

Qualitatively, after a time-period in which an ambient plasma is built up by the beam particles through ionizing collisions with the neutral background, a critical plasma density is reached for which a beam-plasma instability is set up. The waves developed during the instability heat the cold electrons to ionizing energy values and subsequently an avalanche occurs.

Quantitatively, we first calculate the threshold condition for the beam-plasma instability to occur under the conditions of the experiment and also find the growth rate and maximum growth rate of the beam-plasma instability. Second, we balance the rate of plasma production and that of loss through ends. Third, combining the threshold condition and the balance equation we obtain the sought-for relationship between the critical current and the physical parameters, as found in the experiment.

**References**

Bernstein, W., H. Leinbach, P. Kellog, S. Monson and T. Hallinan, J. Geophys. Res., Parametric Dependences and Plasma Wave Characteristics of the Beam-Plasma Discharge at Low Pressures and Magnetic Field Strengths, J. Geophys. Res., 1980, in press.

E - 6HIGHER ORDER FLUID EQUATIONS FOR MULTI-COMPONENT NON-EQUILIBRIUM  
STELLAR (PLASMA) ATMOSPHERES AND STAR CLUSTERS

S. Cuperman and I. Weiss

Department of Physics and Astronomy, Tel Aviv University,  
Ramat Aviv, Israel

M. Dryer

Space Environment Laboratory, ERL, NOAA, Boulder, Colorado,  
U.S.A.

A generalized fluid theory which is required for the description of time-dependent, spatially non-homogeneous, anisotropic, multi-species spherically symmetric systems of particles obeying an inverse-square law of interactions is developed. The resulting equations apply to the expansion of stellar atmospheres (and in particular for the case of the solar wind), stellar systems, as well as controlled thermonuclear devices based on spherical inertial confinement (e.g., laser-pellet interaction, etc.).

The generalization consists of the derivation—starting from the Boltzmann equation—of a higher order, closed system of equations for the moments of the particle velocity distribution,  $f_a$ . Thus, in addition to the familiar equations for the particle density,  $n_a$ , streaming velocity,  $\langle v \rangle_a$ , and temperature,  $T_a$ , the present set of closed equations also includes equations for the heat flux,  $q_a$ , as well as for the fifth moment,  $\epsilon \equiv n_a^{-1} \int (v_r - \langle v_r \rangle)^4 f_a dv = 3(KT_{a,r}/m)^2$  representing the excess (deficiency) of particles in the tail of the distribution function as compared with a Maxwellian particle distribution function. (Here,  $KT_{a,r}$  is the radial random kinetic energy of any specie,  $a$ ). In this formulation, there are three types of deviation from an isotropic Maxwellian which are able to drive the system to a relaxed state, namely, the anisotropy factor  $T_{a,r} - T_{a,\perp}$ , the heat flow  $q_{a,r}$  and the non-thermal tail,  $\epsilon_a$ . This in addition to the differences in the temperature of the various species.) The evolution of a physical system described by such equations exhibits a global, non-local behaviour.

E - 7ON THE STRUCTURE OF THE PARTICLE DISTRIBUTION FUNCTIONS AND THE  
DISPERSION RELATION IN MAGNETIC MIRROR CONFIGURATIONS

L. Gomberoff and S. Cuperman

Department of Physics and Astronomy, Tel Aviv University,  
Ramat Aviv, Israel

The equilibrium particle distribution functions,  $f$  in magnetic mirror configurations are characterized by two anisotropy effects, namely i) an empty cone of low transverse velocity

particles, and ii) a thermal anisotropy,  $T_{\perp}/T_{\parallel} \neq 1$  (parallel and transverse - refer to the direction of the local magnetic field,  $B_0$ ). Each one of these two effects leads to plasma instabilities and consequently the solution of the general dispersion relation is rather difficult.

A careful investigation of the problem reveals the following important points: i) in the case of e.m. cyclotron waves propagating parallel or almost parallel to  $B_0$ , the two effects are additive if  $T_{\perp}/T_{\parallel} > 1$  and the dispersion relation reduces to the simpler and analytically tractable one for a bi-Maxwellian with a modified, effective thermal anisotropy; ii) in the case of unstable e.s. cyclotron waves propagating perpendicular to  $B_0$ , only the loss cone effect is present; iii) in the obliquely propagating case both effects are present and situations can occur in which, due to their reciprocal cancellation, the plasma is stabilized.

## E - 8

### DENSITY OF Cd I AND Cd II EXCITED STATES IN A MULTI-CATHODE-SPOT VACUUM ARC. PART I - SPATIAL DEPENDENCE

S. Shalev and S. Goldsmith  
Department of Physics and Astronomy, Tel-Aviv University,  
Ramat Aviv, Israel

R. L. Boxman  
School of Engineering, Department of Interdisciplinary Studies,  
Tel-Aviv University, Ramat Aviv, Israel

The density of excited states of Cd I and Cd II in a multi-cathode-spot vacuum arc between cadmium electrodes was determined spectroscopically by measuring the absolute intensity of spectral lines. The arc was run between two cylindrical electrodes (diameter 1.2 cm., separation 0.4 cm.). Discharge duration was 1 ms with peak current of 1.2 kA. Excited state densities were studied as a function of time and distance from the cathode. The observations presented here are (1) density measurements, and (2) spatial dependence of excited state populations. No distribution temperature could be assigned as the observed densities could not be fitted to a Boltzman distribution. In addition to a primary density peak near the cathode, a sharp secondary peak was observed for some Cd I and Cd II levels at a distance of 1.2 mm from the cathode for  $t > 0.5$  ms. The second density peak was larger than the first one.

E - 9**DENSITY OF Cd I AND Cd II EXCITED STATES IN A MULTI-CATHODE-SPOT VACUUM ARC. PART II - TEMPORAL DEPENDENCE**

S. Shalev and S. Goldsmith  
 Department of Physics and Astronomy, Tel-Aviv University,  
 Ramat Aviv, Israel

R. L. Boxman  
 School of Engineering, Department of Interdisciplinary Studies,  
 Tel-Aviv University, Ramat Aviv, Israel

The density of excited states of Cd I and Cd II in a multi-cathode-spot vacuum arc between cadmium electrodes was determined spectroscopically by measuring the absolute intensity of spectral lines. The arc was run between two cylindrical electrodes (diameter 1.2 cm., separation 0.4 cm.). Discharge duration was 1 ms with peak current of 1.2 kA. Excited state densities were studied as a function of time and distance from the cathode. The observations presented here are (1) temporal dependence of the excited state densities for selected states of Cd I and Cd II as a function of axial distance from the cathode, (2) HAFW times for the density pulse also as a function of axial position, and (3) spatial and temporal change of excited state density as a function of state excitation energy. We found that the time of peak density is not correlated with the time of peak current (0.25 ms after arc initiation). In Cd II the time of peak density was correlated with the state excitation energy. Along the axis peak time increased with axial distance from the cathode. HAWF of the density pulse also depended on axial position and excitation energy. Population inversion was also observed in Cd II. The inverted population ratios also depended on time.

E - 10

A Flash X-ray System with 0.5mm Source Size Tube.

Z. Segalov, Y. Carmel, S. Eylon, A. Ginzburg and Y. Goren.

Government of Israel Scientific Department, Haifa.

A flash X-ray system was devised for high speed photography of fast moving objects. It consists of a Marx pulse generator driving an X-ray tube having a small source size of 0.5mm (1).

The 30 Joule pulse generator is composed of five stages stacked in series, each negatively charged to 40 KV. When triggering the spark gaps between stages a 200 KV, 3 KA pulse is generated. The Coaxial form of the generator reduces its internal inductance to produce a pulse rise time of a few nanoseconds.

The pulse generator drives through a  $70\Omega$  coaxial cable a vacuum diode in a field emission mode. This diode consists of a conical tungsten anode and a stainless steel sharp edge cathode ring mounted coaxially with the anode. A 0.5 mm X-ray source size was obtained and a 30 nsec pulse duration was measured. At 200 KV a dose rate of  $5 \cdot 10^7$  Roentgen per second was produced at the exit port.

(1) Y. Carmel and S. Eylon, Rev. Sci. Instr. 50, (1979), 1.

## E - 11

Instability of Relativistic Electron Beam in Conical Diode.

Y. Goren, Z. Segalov, Y. Carmel, S. Eylon, and A. Ginzburg.

Government of Israel Scientific Department, Haifa.

Filamentation instability in relativistic electron beams in a conical diode configuration has been observed. Such instability can, in principle, enhance asymmetrical pellet heating in electron pellet inertial fusion devices.

In a conical diode configuration the electron beam is self focused at the anode tip by the combined electric and self magnetic fields (1). High current densities up to  $5 \text{ MA/cm}^2$  were measured. View of the Bremstrahlung X-ray produced by electrons striking the anode shows a filamentation pattern with three to six rotational symmetry in the beam flow. The instability is driven by the perturbed electromagnetic fields in an azimuthal inhomogenous ion sheath generated on the anode surface.

(1) Z. Segalov, Y. Goren, Y. Carmel and S. Eylon, Phys. Lett. 72A, (1979), 435.

THURSDAY MORNING, APRIL 10, 1980  
09:00

FEINBERG A

## F. PHASE TRANSITIONS AND INSTABILITIES

S. Alexander - Hebrew University, Jerusalem - Presiding

### F-1 INVITED

#### FERROMAGNETIC SUPER CONDUCTORS

A. Ron, Technion, Israel Institute of Technology,  
Haifa

### F-2

#### CRITICAL DIFFUSION IN A 2-D ISING MODEL

Y. Achiam

Nuclear Research Centre - Negev, P.O.B. 9001, Beer-Sheva

A model for the critical relaxation in an Ising - like spin system with conserved magnetisation is presented. This model generalises Kawasaki's<sup>1</sup> by allowing any two spins in the system to exchange their values. The model is analysed in two dimensions using the time dependent real space renormalisation group<sup>2</sup>. In order to perform the calculation we used the potential moving approximation suggested by Kadanoff.

We examined the relaxation of the even perturbations (energy like), and showed that there are non-Markoffian corrections which have to be taken into account. We calculated the critical exponent  $z$  which characterises the diffusion near the critical point. We found the value  $z = 3.746$ . Using a near four dimension expansion Halperin et. al.<sup>3</sup> show that an exact value of  $z = 4 - \eta$ , where  $\eta$  is the critical exponent of the correlation function, is expected. This result has been verified using similar exact time dependent renormalisation group transformations in one dimension. The value we found in the present work is in excellent agreement with the expected  $z = 3.75$ .

1. K. Kawasaki Phys. Rev. 145, 224 (1966).
2. Y. Achiam and M. J. Kosterlitz Phys. Rev. Lett. 41, 128 (1978).
3. B. I. Halperin, P. C. Hohenberg and S. K. Ma Phys. Rev. B10, 139 (1974).

F - 3

## CROSSOVER FROM FIRST-ORDER TO CONTINUOUS TRANSITION INDUCED BY SYMMETRY-BREAKING FIELDS.

M. Kerszberg and D. Mukamel

Department of Nuclear Physics, Weizmann Institute of Science, Rehovot.

We study model Hamiltonians which do not flow to stable fixed points under renormalization-group transformations, either because an existing stable fixed point is not accessible [e.g. the  $n = 2$  cubic model<sup>1</sup>], or because there is no stable fixed point at all [e.g. models associated with <sup>2</sup>UO<sub>2</sub> or <sup>3</sup>CeS]. This is generally interpreted as indicating a first order transition. By applying suitable symmetry-breaking fields  $g$ , however, one may restore accessibility of a stable fixed point and thus induce a crossover to a continuous transition. We study this phenomenon, using perturbative techniques at large field  $g$ , and relying on the indications of mean-field theory. We find phase diagrams exhibiting tricritical points, critical end-points and fourth-order critical points. Other possibilities that might occur in UO<sub>2</sub> or in CeS will be discussed.

1. M.Kerszberg and D. Mukamel, Phys. Rev. Lett. 43, 293 (1979)
2. P. Bak, S. Krinsky and D. Mukamel, Phys. Rev. Lett. 36, 52(1976).
3. D. Mukamel and D.J. Wallace, J. Phys. C13, L851 (1979).

\* Work supported in part by the U.S.-Israel Binational Science Foundation (BSF), Jerusalem.

F - 4

## COMMENSURATE-INCOMMENSURATE TRANSITION IN AN ADSORBED LAYER

M. Ya. Azbel

Department of Physics and Astronomy, Tel Aviv University, Ramat Aviv, Israel

A model for a commensurate-incommensurate phase transition is presented. It allows for an exact determination of the adsorbed atoms ground state. When the concentration of adsorbed atoms increases, a set of ground state commensurate-incommensurate transitions takes place. It is related to the decomposition of  $2R_S/R_a$  into the continuous fraction,  $R_S$  and  $R_a$  ( $R_S < R_a < 2R_S$ ) being the sizes of substrate and adsorbed atoms.

F-5

## NON-UNIVERSAL SPIN SYSTEMS ON UNION-JACK LATTICES

M. Gitterman

Department of Physics, Bar-Ilan University, Ramat-Gan

It is shown that both the union-jack two-dimensional lattice models with pair interactions only, and also models with three-spin interactions, may exhibit non-universal behaviour, namely, the critical indices depend on the interaction energy.

F-6RENORMALIZATION GROUP APPROACH TO THE MAGNETIC PHASE TRANSITION IN SOLID  $^3\text{He}$  (\*)

Y. Shnidman and D. Mukamel

Department of Nuclear Physics, Weizmann Institute of Science, Rehovot.

A renormalization group (RG) approach is proposed to account for the qualitative features of the magnetic phase transition in solid  $^3\text{He}$ . The study suggests that the first order transition at 1.1 mK may be associated with a transition from a paramagnetic to a type II antiferromagnetic ( $\text{AF}_2$ ) phase. The  $n=6$  - component Landau-Ginzburg-Wilson (LGW) Hamiltonian corresponding to this transition is constructed. The model is found to exhibit no stable fixed point in  $d=4-\epsilon$  dimensions, indicating a first order transition. The relation of this model to microscopic models such as the Heisenberg model with nearest and next-nearest-neighbour interactions and models with four-spin interaction is discussed. The effect of symmetry breaking magnetic fields on the order of the transition is also considered.

(\*) Work supported in part by a grant from the US-Israel Binational Science Foundation, Jerusalem.

F-7

## THERMODYNAMIC STABILITY AND PHASE TRANSITIONS IN SYSTEMS WITH A CHEMICAL REACTION

M. Gitterman

Department of Physics, Bar-Ilan University, Ramat-Gan

V. Steinberg

Department of Physics, Tel-Aviv University, Ramat-Aviv

The general stability conditions for systems with a chemical reaction<sup>1</sup> are considered. In addition to the usual critical



phenomena, a new chemical instability appears which is connected with the multiple solution of the law of mass action. As a result of the first-order phase transition, the system separates into several phases with different reactant concentrations. Examples of isomerization and ionization reactions are considered. In the latter case, as the fraction of highly ionized phase increases, the conductivity of the system becomes metallic. Experimental evidence for the predicted instability has been obtained in recent calorimetric measurements on the sodium-ammonium solution.<sup>2</sup>

- <sup>1</sup>M. Gitterman, V. Steinberg, Phys. Rev. A20, 1236, 1979, J. Chem. Phys. 69, 2763, 1978; 65, 847, 1976; Chem. Phys. Lett. 57, 455, 1978.
- <sup>2</sup>A. Voronel, V. Steinberg, D. Linskii "Calorimetric investigation of metal-non-metal transition in sodium-ammonium solution", IPS Conference, 1980.

## F - 8

### RAYLEIGH-BENARD INSTABILITY IN A SUPERFLUID SOLUTION

V. Steinberg  
Department of Physics and Astronomy, Tel Aviv University,  
Ramat Aviv, Israel

The He<sup>3</sup>-He<sup>4</sup> solution below the  $\lambda$ -line represents a very unusual Rayleigh-Benard system as owing to physical nature of a mixture as well as to a very wide variation of the parameters affecting the onset of the convection.

The hydrodynamic stability analysis of horizontal layer of He<sup>3</sup>-He<sup>4</sup> superfluid mixture is presented in the Boussinesq approximation for both stationary and oscillatory convection. From the viewpoint of stability this mixture resembles both binary mixture with the abnormal Soret effect [1] and a compressible fluid [2] because a superfluid current is involved. For certain parameter values, we predict a direct transition to oscillatory convection which should be observable under realistic conditions.

- [1] V. Steinberg, J. of Applied Math. and Mechanics, 35, 335, 1971.
- [2] M. Gitterman, V. Steinberg, J. of Applied Math. and Mechanics, 34, 305, 1970.

F - 9

## NEW ASPECTS OF NEMATIC FLOW PATTERNS

S. I. Ben-Abraham

Physics Department, Ben-Gurion University, 84 120 Beer-Sheva

Under suitable boundary conditions and in the conduction regime, a thin layer of a nematic in an electric field will develop a characteristic roll-type flow pattern. Optically this is manifested as a "domain" pattern. Squint is a nonlinear feature peculiar to liquid crystals; it is the skewing of the rolls due to the differences in the Frank elastic constants.<sup>1</sup> A refined discussion of squint is presented in terms of the director angle  $\phi$  rather than the pattern curvature. Squint results from the terms  $2(k_{33} - k_{11})\{\sin(2\phi)(\partial^2\phi/\partial x\partial y) + \cos(2\phi)(\partial\phi/\partial x)(\partial\phi/\partial y)\}$  in the distortion torque density. Squint occurs both across and along the sample. Some striking patterns with squint have been observed by Faetti et al.<sup>2</sup> Some possible novel effects due to variations in the boundary conditions will also be discussed.

1. S. I. Ben-Abraham, J. Physique 40, 229 (1977).
2. S. Faetti, L. Fronzoni, P. A. Rolla and G. Stoppini, Lett. Nuovo Cimento 17, 475 (1976).

F - 10METALLIC - NONMETALLIC PHASE COEXISTENCE ABOVE THE CRITICAL POINT OF Na-NH<sub>3</sub> SOLUTION.

V. Steinberg, A. Voronel and D. Linsky

Department of Physics and Astronomy, Tel Aviv University, Ramat Aviv, Israel.

U. Schindewolf

Institute of Phys. Chemistry, University of Karlsruhe, Karlsruhe, West Germany.

Heat Capacity ( $C_p, x$ ) of three compositions ( $X > X_c$ ) of Na-NH<sub>3</sub> solution have been measured in interval 200 + 300K. All three curves have shown anomalies above the liquid-liquid critical point ( $T > T_c = 232K$ ). These anomalies can be considered as jumps of  $C_p$  near the borders of two-phase equilibrium of metallic and non-metallic liquid phases which have been predicted by M. Gitterman and V. Steinberg [1]. The coexistence line of this transition has been traced until room temperature.

[1] M. Gitterman, V. Steinberg, Phys. Rev. a20, 1236, 1979.

F - 11SPECIFIC HEAT OF A 5%  $^3\text{He}$ - $^4\text{He}$  SOLUTION UNDER PRESSURE\*E. Polturak<sup>+</sup> and R. RosenbaumTel Aviv University, Department of Physics and Astronomy,  
Ramat Aviv, Israel

Specific heat measurements on a 5.0%  $^3\text{He}$ - $^4\text{He}$  solution have been made under pressure at very low temperatures of 13 mK to 80 mK in order to obtain the specific heat Fermi temperature,  $T_F^{\text{sh}}$ , and the specific heat effective mass,  $m^{\text{sh}}$ ; these quantities appear in the table below. The specific heat theory of H. Brucker and Y. Disatnik has been used to extract the zero concentration specific heat mass  $m_0$ ;<sup>1,2</sup> The zero concentration effective mass is a measure of the  $^4\text{He}$  density profile around the  $^3\text{He}$  atom in the  $^4\text{He}$  superfluid;  $m_0$  does not include interactions between the  $^3\text{He}$  quasiparticles. Values of  $m_0$  appear below:

Pressure (atm.)	$T_F^{\text{sh}}$ (K)	$m^{\text{sh}}/m_3$	$m_0/m_3$
0	.327±.007	2.49 ± .07	2.34
10	.313±.006	2.76 ± .06	2.65
20	.294±.006	3.06 ± .06	2.87

\* This work was partially supported by the United States-Israel Binational Foundation (BSF), Jerusalem.

+ Present address: Cornell University, Laboratory for Atomic and Solid State Physics, Clark Hall, Ithaca, New York, 14850.

<sup>1</sup> Y. Disatnik and H. Brucker, J. Low Temp. Phys. 7, (1972) 491.

<sup>2</sup> H. Brucker and Y. Disatnik, Low Temperature Physics-LT-13, vol.1 (Plenum Press, New York, 1974) 598.

F - 12MAGNIFICATION OF SINGULARITIES OF THE THERMODYNAMIC QUANTITIES  
NEAR CRITICAL POINTS IN THE PRESENCE OF A CHEMICAL REACTION

M. Gitterman

Department of Physics, Bar-Ilan University, Ramat-Gan

V. Steinberg

Department of Physics, Tel-Aviv University, Ramat-Aviv

Systems undergoing chemical reactions are those where a constant chemical potential is the only possible way of measurement. Therefore, such measurements will give the "ideal" critical indices. Using a catalyst, one can find a magnification of singularities in the presence of a chemical reaction comparable with the "frozen" reaction. We consider the case of a mixture with one chemical reaction, as well as liquid-gas and liquid-liquid critical phenomena in solutions where the solvent does not participate in chemical reaction. Changes of critical indices for systems with and without chemical reaction are obtained.

F - 13PROBABLE ELECTRONIC TRANSITION IN  $K_2Cs$  COMPOUND AT LOW  
TEMPERATURE

V. Steinberg, A. Voronel, T. Sverbilova, L. Peretsman  
Department of Physics and Astronomy, Ramat Aviv, Tel-Aviv  
University, Israel.

A new phase transition in an intermetallic compound  $K_2Cs$  has been found at about 110K. Both X-ray scattering and resistivity measurements show an enormous change in

volume ( $\frac{\Delta V}{V} \sim 0.14$ ) at the transition temperature. The samples of  $K_2Cs$  appear to be extremely soft and they recover completely after the strong deformation. In the present paper we suggest that these effects are connected with the electronic transition in Cs atoms discussed by R.L. Sternheimer [1].

[1] R.L. Sternheimer, Phys. Rev., 78, 235, 1950.

F - 14

## MEMORY EFFECTS IN THE MOTION OF SUSPENDED PARTICLE IN A TURBULENT FLUID

M. Gitterman

Department of Physics, Bar-Ilan University, Ramat-Gan

V. Steinberg

Department of Physics, Tel Aviv University, Ramat-Aviv

The non-instantaneous behavior of the velocity correlation function for a turbulent fluid leads to memory effects in the equation of motion of a particle suspended in such fluid. This effect is a direct consequence of the fluctuation-dissipation theorem, which connects the correlation properties of the random force with a memory function. As a result, the equation of motion of a suspended particle in a turbulent flow is an integro-differential rather than a differential equation, and the diffusion coefficient of a suspended particle and that of a fluid do not coincide even in the simplest model. The velocity correlation function of a particle and its diffusion coefficient are found for a simple model.

THURSDAY MORNING, APRIL 10, 1980  
09:00

FEINBERG D

## G. PLASMA PHYSICS II

D. Salzmann, Soreq Nuclear Research Center - Presiding

### G-1 INVITED

WAVE PHENOMENA IN LASER FUSION

E. Shalom, Soreq Nuclear Research Center

### G-2

INCIDENCE ANGLES OF ELECTRONS IN THE PINCH REGION OF LARGE ASPECT RATIO RELATIVISTIC ELECTRON BEAM DIODES.

Y. Maron

Department of Physics, Weizmann Institute of Science

It is well known<sup>1,2)</sup> that in large aspect ratio diodes the net velocity of the electrons converging towards the pinch region is essentially parallel to the anode plane. In this work, pinhole bremsstrahlung photography was used to measure the angular distribution of electrons hitting the anode in the pinch region. It was found that electron velocity directions change significantly after collapsing into the pinch region, transforming to nearly parallel to the diode axis. At the pinch center the distribution is peaked in the direction of the diode axis, where the incidence angles of most of the electrons are limited to few tens of degrees. Up to the pinch outer radius the angular distribution of the electrons maintains its shape but the average direction points towards the pinch axis at angles of less than  $10^\circ$ . In most of the shots aluminum anodes were used. However, similar results were obtained with tantalum anodes. The measured angular distribution of the electrons show that the angular distribution of the bremsstrahlung radiation is nearly the same for each point of the pinch region. Thus, pinhole photography can be reliably used to determine current density profiles in this region. From these results and from simple calculations of electron trajectories in the pinch region it is inferred that either a strong axial electric field at the anode vicinity or a radial electric field balancing the magnetic field in the pinch region prevails in this region.

- 1) S.A. Goldstein, R.C. Davidson, J.G. Siambis, and R. Lee, Phys. Rev. Lett. 33, 1471, (1974).
- 2) A.E. Blaugrund, G. Cooperstein, and S.A. Goldstein, Phys. Fluids, 20, 1185 (1977).

G - 3

**MODIFICATION OF ENERGY DEPOSITION IN FOIL ANODES OF PINCHING  
RELATIVISTIC ELECTRON BEAM DIODES BY EXTERNAL  $B_z$  FIELDS.**

Y. Maron and A.E. Blaugrund  
Department of Physics, Weizmann Institute of Science.

Relativistic electrons emerging from the pinch region of a diode through a thin foil anode tend to form a virtual cathode which causes the electrons to reflex. However, because of the 3-dimensional shape of this virtual cathode only a small fraction of the reflexing electrons return to the anode foil in the pinch region. We have devised a method for confining the electrons to the anode. A thin wire is attached axially to the center of the foil on the outside of the diode. A relatively fast capacitor discharge circuit passes a current up to 150 kA through the wire and then through the anode back to ground. Electrons emerging from the foil encounter a strong  $B_z$  field around the wire and are forced into Larmor trajectories with radii around 0.1 mm. Assuming space charge neutrality the electrons are also subjected to a  $\nabla B$  drift motion. Pinhole bremsstrahlung and laser shadow photographs of the foil and wire were taken. When the direction of the magnetic field was the same as that of  $B_z$  inside the diode energy was deposited in the wire. On the part of the wire close to the anode the specific energy density increased with increasing external current. When a thin hollow cylinder was used instead of a wire the specific energy deposition was at least as high as in the adjacent foil anode. When the external current is reversed the  $\nabla B$  drift motion forces the emerging electrons to return to the foil. This phenomenon was verified by observing that in this case almost all the electrons are stopped in the anode rather than to propagate down the drift tube. Their energy is deposited in the foil both inside and outside the regular pinch. Laser photography showed increased foil expansion velocity just outside the pinch region. The integral energy deposition at the anode foil is at least twice that obtained in regular pinch shots. Such confinement of the electrons to the anode vicinity may amplify the ion current in the diode.

G - 4

**Z DEPENDENT ABSORPTION AND STIMULATED BACKSCATTER PROCESS  
IN LASER PRODUCED PLASMAS**

S. Jackel, H.M. Loebenstein, A. Zigler, H. Zmora and  
S. Zweigenbaum, Soreq Nuclear Research Center, Yavne 70600,  
Israel

Low and high atomic number targets were irradiated at normal and oblique incidences with high focused intensity, 2.5 nsec duration 1.06 $\mu$ m laser pulses. Calorimetry and spectroscopy of  $\omega$  and  $2\omega$  light reflected back into the focusing lens was

performed. Results show a dramatic reduction in the specularly reflected light from high atomic number targets. Brillouin backscatter was observed throughout the range  $10^{14}$  -  $10^{16}$  W/cm<sup>2</sup>.  $2\omega$  spectra indicated the presence of an electron-ion decay instability with a threshold at  $2 \times 10^{15}$  W/cm<sup>2</sup>.

## G - 5

### EFFECT OF PULSE DURATION AND POLARIZATION ON MOMENTUM AND ENERGY TRANSFER TO LASER IRRADIATED TARGETS (1)

B. Arad, S. Eliezer, S. Jackel, A.D. Krumbein, H.M. Loebenstein, D. Salzmann, A. Zigler, H. Zmora and S. Zweigenbaum

Polished aluminum targets were irradiated with 1.06 $\mu$ m laser pulses of 60 picosecond and 2.5 nanosecond duration at oblique incidence and with a high focussed intensity of between  $10^{14}$  and  $10^{16}$  Watt/cm<sup>2</sup>. Laser light of both  $\pi$  and  $\sigma$  polarization was used in the experiments. The primary diagnostic was a torsion pendulum which measured the momentum imparted to the target while supporting data was provided by charge collectors (Faraday cups). The main purpose of this work was the experimental determination of the resonant absorption contribution to the momentum imparted to targets irradiated with short and long duration laser pulses.

Resonant absorption contributions were clearly observed for the short pulses - the  $\pi$  polarized light giving 35% more momentum transfer to the target. This is in agreement with resonant absorption experiments performed elsewhere. For the long pulses, however, no polarization dependent or angle of incidence effects were observed. This may be the result of small scale rippling or turbulence at the critical surface. The momentum coupling efficiency was found to be independent of laser intensity for the short pulses and to decrease by more than a factor of two for the long pulses over the laser intensity range studied. This behavior appears to be a consequence of corona temperature variations with incident light intensity.

### References

(1) Accepted in Phys. Rev. Letters.



G - 6**ON THE DEPENDENCE OF IGNITION THRESHOLD ON THE BURN MODEL IN A DT PELLETT.**

D. Havazelet, D. Shvarts  
Nuclear Research Center-Negev, POB 9001, Beer-Sheva

The ignition of a compressed DT Pellet is achieved by producing a hot spot at the pellet's center[1]. A burning front is thus created and is propagating outward. It is possible to draw a threshold curve for the propagation of the burning front on the  $\rho R$  vs  $T$  plane of the hot spot[1]. This threshold curve depends on the burn model.

Some aspects of different models dealing with transport of Radiation,  $\alpha$  particles and electron conductivity and their influence on the threshold curve are discussed.

1. R. Kidder, Nucl. Fus. 19, 223 (1979).

G - 7**HARD X-RAY AND FAST IONS PRODUCTION BY FAST ELECTRONS IN LASER-PRODUCED PLASMAS**

D. Shvarts, T. Bar-Noy  
Nuclear Research Center-Negev, POB 9001, Beer-Sheva

J. Virmont  
Laboratoire de Physique des Milieux Ionises  
Ecole Polytechnique, Palaiseau, France

The energy losses of fast electrons, created by laser plasma interaction, to the accelerated corona, change their effective energy when they enter the denser core[1].

Therefore, the effective temperature inferred from the hard x-ray spectrum, produced by the fast electrons in the denser region, may be substantially lower than the source temperature.

The dependence of the effective x-ray temperature and the fast ion production on various target and laser parameters will be discussed.

1. D. Shvarts, C. Jablon, I. Berenstein, J. Virmont, P. Mora; Nucl. Fus. 19, 1457 (1979).

G - 8THE EFFECT OF FAST ELECTRONS ON THE MOMENTUM  
COUPLING IN LASER - PLASMA INTERACTION

T. Bar-Noy, M. Sapir, D. Shvarts  
Nuclear Research Center-Negev, POB 9001, Beer-Sheva

The momentum imparted by a laser beam to a target depends on the amount of fast electrons produced and their transport.

Fast electrons preheat the target and lose energy to accelerate the outer expanding corona.

The dependency of the momentum coupling efficiency on the laser intensity and pulse length has been investigated numerically and will be presented.

G - 9

## A MODIFIED DIFFUSION TREATMENT OF FAST, LONG-MEAN-FREE-PATH ELECTRONS IN LASER PRODUCED PLASMA

M. Strauss, J. Oreg, D. Shvarts  
Nuclear Research Center-Negev, POB 9001, Beer-Sheva

The transport of suprathermal electrons dominates the behaviour of the laser produced plasma[1]. Most of the present codes[2,3] used the usual flux-limited diffusion treatment. However, this approximation is not adequate in the outer underdense corona where the collisional mean-free-path is longer than the spatial scale length. In that region the transverse component of the electron angular distribution function is bigger than the radial one, especially for low Z plasmas. Thus a large fraction of suprathermal electrons remain in the low density region until significant radial velocity component is acquired due to cumulative scattering. A modified diffusion coefficient which takes into account this effect is derived.

Comparison of this model with the usual diffusion model, a new moment method which was developed and available Monte-Carlo results will be presented.

1. W.L. Kruer, *Comm. Plasma Phys.* 5, No.3, 69 (1979).
2. D. Shvarts, C. Jablon, I.B. Bernstein, J. Virmont and P. Mora, *Nucl. Fus.* 19, 1457 (1979).
3. G.B. Zimmerman, Lawrence Livermore Laboratory UCRL-74811 (1973).

G - 10

CELL THEORY AND THE  $\frac{1}{T}$  PERTURBATION EXPANSION  
 IN RELATION TO ISOSTRUCTURAL PHASE TRANSITION  
 DUE TO CORE COLLAPSE\*

M. Giv'on  
 Dept. of Phys. Ben-Gurion University, Beer-Sheva

Y. Rosenfeld  
 Nuclear Research Center-Negev, POB 9001, Beer-Sheva

R. Thieberger  
 Nuclear Research Center-Negev, POB 9001, Beer-Sheva

A  $\frac{1}{T}$  expansion of the difference between the cell theory calculated free energy of a square well system and a hard core system is presented. With this expansion we compare two methods for the calculation of phase diagrams.

A fair agreement between the cell theory and the  $\frac{1}{T}$  perturbation expansion is obtained.

\*M. Giv'on, Y. Rosenfeld and R. Thieberger  
 Chem. Phys. Lett. (to be published)

G - 11

STATICS AND THERMODYNAMICS OF STRONGLY  
 COUPLED MULTICOMPONENT PLASMAS

Y. Rosenfeld  
 Nuclear Research Center-Negev, POB 9001, Beer-Sheva

A description of strongly coupled plasmas, in which the direct correlation functions,  $c_{ij}(r)$ , are obtained by simple scaling from a universal function, is derived and found to be in full agreement with available computer simulation data, which it thus extends for arbitrary mixtures. It is thermodynamically consistent with the "ion sphere" charge averaging prediction for the enhancement factors for nuclear reactions rates, the results for which confirm the universality of the bridge functions for mixtures [1].

(1) Y. Rosenfeld, Phys. Rev. Lett. 44, 146 (1980).

THURSDAY MORNING, APRIL 10, 1980  
09:00

Phys. Bldg.  
Large Lect.  
Hall

## H. THIN FILMS

G. Deutcher - Tel Aviv University - Presiding

H-1 INVITED

THE MORPHOLOGY, PHASE CONSTITUTION AND TEXTURE  
OF POLYCRYSTALLINE THIN FILMS

U. Admon, Nuclear Research Center, Negev

H - 2

Electron Diffraction Study of Some Epitaxial Films and Phase  
Transitions in the Cu-S System.

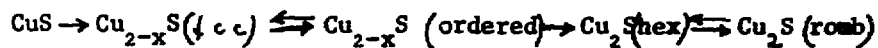
M. M. Kazinets

Institute of Physics, Baku, U.S.S.R.

Monocrystalline films of  $\text{Cu}_{2-x}\text{S}$  were obtained by evaporation  
in high vacuum of a synthesized compound of  $\text{Cu}_{1.9}\text{S}$  onto the  
(001) face of NaCl single crystals held at  $350 - 400^\circ\text{C}$ .

The transmission electron diffraction patterns show that the  
 $\text{Cu}_{2-x}\text{S}$  has a cubic superstructure and an orientation parallel  
to that of the substrate. The film is composed of crystals  
with superstructure domains in two different orientations.

Phase transitions of :



were observed on polycrystalline films using the kinematic  
electron diffraction method.

H - 3

## THE EFFECT OF LIGHT-INDUCED SELECTIVE CORROSION ON THE PROPERTIES OF Cd-CHALCOGENIDES BASED PHOTOELECTROCHEMICAL CELLS

R. Tenne, G. Hodes, J. Manassen - Plastics  
 D. Cahen - Structural Chemistry  
 The Weizmann Institute of Science, Rehovot

Light-induced selective corrosion of both single crystal and polycrystalline Cd-chalcogenides photoelectrodes has a large positive effect on the performance of solar cells, based on these electrodes<sup>(1)</sup>. It is found that pits of the size of  $0.1\mu$  are formed on the surface of the semiconductor during the photocorrosion. As a result the treated surface reflects  $\sim 10\%$  less photons than prior to treatment. In addition, the larger surface area of the junction results in an increase of the (dark) forward current through the Schottky barrier. Also, the stability of the photoelectrode is improved remarkably which substantiates our findings concerning the influence of surface area on photoelectrode stability<sup>(2)</sup>.

The large increase in the short circuit-current and the decrease in the dark current close to flat band situation, in polycrystalline electrodes, indicates that a decrease in the density of shallow surface states (close to the conduction band), may occur as well.

1a) G. Hodes, Nature (London) in press.

1b) R. Tenne and G. Hodes, submitted.

2) D. Cahen, G. Hodes, J. Manassen, J. Electrochem. Soc. 125, 1623 (1978).

H - 4

## CRYSTALLIZATION OF AMORPHOUS Dy-Fe THIN FILMS

L. Shikhmanter and M. Talianker  
 Department of Materials Engineering  
 Ben-Gurion University of the Negev, Beer-Sheva

M.P. Dariel  
 Department of Materials Engineering and  
 Nuclear Research Center-Negev

The crystallization behavior of amorphous Dy-Fe thin films was investigated by transmission electron microscopy and by electron diffraction. Amorphous Dy-Fe films were prepared by vapor deposition at  $10^{-6}$  torr. The films were heated in situ in a JEOL 200 electron microscope and ring electron diffraction patterns together with bright- and dark field images obtained. Alloys with 25 at.%, 35 at.% and 55 at.% Dy were examined. The diffraction pattern from the as prepared films shows a broad diffuse halo. At 100 C,  $DyH_2$  is formed due to the prevalent presence of  $H_2$  in the residual gas. At

150 C, the dihydride decomposes and stable sesquioxide  $Dy_2O_3$  appears. At 250 C, small Fe crystallites, approximately 100 Å in size, precipitate in the 25 at.% Dy alloy. In the 35 at.% Dy alloy, the first Fe crystallites appear at 350 C. The further heating of these alloys causes the growth of both the iron and oxide phases. When the Dy content increases to 55 at.%, the Fe crystallites appear only at 500 C. At 700 C, the formation of metallic Dy crystallites was observed.

The results of this study indicate that the crystallization process in amorphous thin films is not in accordance with the equilibrium Fe-Dy phase diagram. The intermetallic compounds  $DyFe_2$ ,  $DyFe_3$  etc. do not crystallize and merely the separation of metallic Dy and Fe phases was observed.

#### H - 5

#### Calculation of the phase diagram of the Pb-Sn-Te system in the (Pb+Sn)-rich region.

S. Szapiro, N. Tamari and H. Shtrikman.

Soreq Nuclear Research Centre, Yavne, Israel.

The phase diagram of the Pb-Sn-Te system in the (Pb+Sn)-rich region was calculated using the modified model<sup>1)</sup> of regular associated solutions. The calculations were based on experimental values determined by differential thermal analysis (DTA) and liquid phase epitaxy (LPE) techniques. The calculated liquidus temperature and solidus composition surfaces show good agreement with our measured values.

1) S. Szapiro, J. Phys. Chem. of Solids, in press.

H - 6EFFECT OF SUBSTRATE TEMPERATURE ON PERCOLATION THRESHOLD OF  
CO-EVAPORATED Al-Ge FILMS

A. Kapitulnik, M. L. Rappaport, G. Deutscher  
Department of Physics and Astronomy, Tel-Aviv University,  
Ramat-Aviv, Israel

Preliminary measurements indicate that the percolation threshold  $x_c$  of 3-dimensional (3-D) co-evaporated Al-Ge mixtures can be drastically influenced by substrate temperature. Previous results on room temperature substrates gave  $x_c(3D) = 55 \text{ vol.}\%$ .<sup>1</sup> New measurements on samples prepared on identical substrates at  $\sim 180^\circ\text{C}$  show  $x_c(3D) < 28 \text{ vol.}\%$ . An explanation will be given in terms of the film thickness and the micro-structure of the Al and Ge.

1. G. Deutscher, M. Rappaport, and Z. Ovadyahu,  
Solid State Comm. 28, 503 (1978).

## H-7 INVITED

## OPTICAL ANALYSIS OF THIN FILMS

J. Shamir, Israel Institute of Technology, Haifa

H - 8VARIATION OF THE OPTICAL PROPERTIES OF AMORPHOUS SILICON DURING  
CRYSTALLIZATION

M. Janai

Technion, I.I.T., Haifa 32000, Israel

Amorphous silicon films were prepared on fused silica substrates by pyrolytic decomposition (CVD) of silane at the temperature range  $550^\circ\text{C}$  to  $675^\circ\text{C}$ . The films were annealed at various constant temperatures. X-ray diffraction, infra-red reflectance and visible transmittance spectra were measured as a function of annealing time. The results suggest that crystallization starts at individual crystallization centers. The microcrystallites expand till their boundaries touch each other, at which stage the crystallization kinetics changes. The optical properties of the films during crystallization are interpreted by the effective media theory, assuming a composition of two media having dielectric constants of amorphous silicon and crystalline silicon

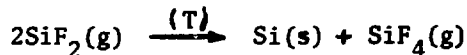
respectively. Substrate effects are discussed. At photon energies between 1.8 eV and 2.6 eV the absorption of the amorphous phase is 1.5 orders of magnitude higher than that of the crystalline phase, which implies that laser annealing at these photon energies may be particularly efficient, since the light is selectively absorbed in the amorphous regions.

### H - 9

#### PROPERTIES OF AMORPHOUS SILICON FILMS PREPARED BY CVD OF SiF<sub>2</sub>

M. Janai, R.B. Weil, K. Levin and B. Pratt  
Technion-Israel Institute of Technology, Haifa 32000, ISRAEL

Amorphous silicon films were prepared by the reaction



in the temperature range  $500^\circ\text{C} \leq T \leq 750^\circ\text{C}$ . The concentration of fluorine in the films, the visible and infrared absorption spectra, the dark dc and ac conductivity and the photoconductivity of the films were measured. The films exhibit generally optical and electronic properties similar to those found in amorphous silicon films prepared by CVD of silane. The films contain between 0.5 and 1.5% fluorine. The dark dc resistivity is  $\sim 10^6 \Omega \cdot \text{cm}$  and it decreases exponentially with increasing temperature with an activation energy of 0.5 eV. The photoconductivity at a light intensity of  $0.1 \text{ w/cm}^2$  is of the order of magnitude of the room-temperature dark conductivity. The photoconductivity exhibits a fast and a slow component. The magnitude of the slow component depends linearly on the light intensity and it varies with temperature, which is characteristic to the photoconductivity in amorphous semiconductors containing a high distribution of gap states. The correlation between preparation parameters and the film properties will be discussed.

### H - 10

#### DIMENSIONAL EFFECTS ON I-V CHARACTERISTICS OF Pb-Ge SUPERCONDUCTING MICROBRIDGES

A. Palevsky, G. Deutscher, and M.L. Rappaport  
Dept. of Physics and Astronomy, Tel-Aviv Univ., Ramat-Aviv.

Microbridges  $\sim 1 \mu\text{m} \times 1 \mu\text{m}$  and  $465 - 775 \text{ \AA}$  thick were formed of co-evaporated Pb-Ge mixtures by the photolithographic technique known as "lift-off". Power law dependences on the metallic volume concentration  $x$  were found for the normal state conductivities,  $\sigma = \sigma_0(x-x_c)^t$ , and the critical current density,  $j_c = j_{c0}(x-x_c)^v$ . The value of  $t$  measured, 0.9, is in agreement with previous work<sup>1</sup> and



indicates that the films were 2-dimensional (2-D). The values of  $v$  are larger than  $t$  but depend on the criterion for critical current. The coefficients  $\sigma_0$  and  $j_{c0}$  and the critical concentrations  $x_c$  depend on thickness,  $\sigma_0$  and  $j_{c0}$  increasing and  $x_c$  decreasing<sup>2</sup> (towards its 3-D value 0.15) with increasing thickness. The I-V characteristics at 4.2K and at 2.0K cannot be explained by the usual models for microbridges (RSJ, flux, creep, phase slip) and may indicate the presence of thermally excited "topological excitations" (vortices).

1. G. Deutscher and M. Rappaport,  
J. Physique Lett. 40, L - 219 (1979)
2. See following abstract.

#### H - 11

##### SPUTTERED HYDROGENATED AMORPHOUS Si ALLOYED WITH Al.

M. Dayan, N. Croitoru and Y. Lereah

Department of Electronic Devices and Electromagnetic  
Radiation, School of Engineering, Tel Aviv University,  
Ramat Aviv, Tel Aviv, Israel .

Hydrogenated amorphous silicon (a-Si:H), prepared by glow-discharge decomposition of silane, or by sputtering in an argon-hydrogen atmosphere, is a material which has gained wide interest because of possible future applications. This material is known for its low density of defect states, and can therefore be doped. Alloying and doping with different elements have been reported. We report here on a simple method of fabrication and the electrical and structural properties of a-Si : H doped with Al. The interesting feature of this system is that it retains the amorphous structure of a-Si up to very high Al concentration (27at%), where the electrical resistivity has decreased by many orders of magnitude to the lowest value observed to date for doped a-Si :H . Al crystallization appears for concentration higher than 27 at. % , accompanied by a non-monotonic behaviour of the resistivity as a function of Al concentration.

H - 12

PHOTORESPONSE MEASUREMENTS AS A TOOL FOR EVALUATING  
Cd-CHALCOGENIDE-BASED PHOTOELECTROCHEMICAL SYSTEMS.

Y. Mirovsky, D. Cahen, G. Hodes, J. Manassen, and R. Tenne  
Weizmann Institute of Science, Rehovot.

Illumination of the interface between n-Cd-chalcogenide and a polysulfide solution produces a photovoltaic effect, which can be used to construct photoelectrochemical devices. (Bull. Isr. Phys. Soc. 24, 27-28 (1978)).

Photoresponse measurements were performed on this system, using modulated optical excitation and phase-sensitive detection, thus enabling measurement of the true anodic photocurrent. In this way several physical parameters can be obtained in situ, i.e. without the need of modifying the semiconductor electrode. These parameters, which are determined as a function of applied electrode potential, include  $V(\text{FB})$  - the flat-band potential of the system,  $N(\text{D})$  - the donor doping concentration, and  $L(\text{p})$  - the hole diffusion length, all of which bear directly on optimization of photoelectrochemical solar cells. The dependences of in-bandgap and sub-bandgap photoresponse on applied bias are different and our results will be discussed in the framework of the Gärtner model and others.

H - 13

## 2-D TO 3-D PERCOLATION TRANSITION IN Pb-Ge FILMS

G. Deutscher and M. L. Rappaport  
Department of Physics and Astronomy, Tel-Aviv University,  
Ramat-Aviv, Israel.

Very plausible arguments give  $x_c(3\text{D}) = 15 \text{ vol.}\%$  as the critical concentration for percolation in a 3-dimensional (3-D) sample. Symmetry demands that  $x_c(2\text{D}) = 50 \text{ area}\%$  in 2-D. We have measured the transition from 2-D to 3-D critical concentrations in Pb-Ge co-evaporated films which had previously been shown<sup>1</sup> to have the random structure required in the above arguments. The

method assumes that any film of finite thickness  $d$  is 2-D at the percolation threshold, and thus that all films of the same materials prepared under the same conditions have, at the percolation threshold, the same resistance per square, regardless of thickness. The results confirm calculations which find that  $\chi_c(d) - \chi_c(3-D) \propto d^{-g}$  where  $g \sim 1$ .

1. G. Deutscher, M. Rappaport and Z. Ovadyahu, Solid State Comm. 28, 503 (1978).

#### H - 14

#### EVALUATION OF THIN FILM OVER-ETCHING IN MICROELECTRONICS

A. Peled & M. Haspel, ELTA Electronics, P.O.B. 330, Ashdod.

The problems and techniques of producing thin films for microelectronics are being addressed with ever increasing sophistication.<sup>(1)</sup> Much attention has been given to the generation of dense patterns, due to improvements in photolithographic techniques. Etching of the patterns is usually done by the wet chemical method. This method is the least expensive and has been in use for a long time.<sup>(2)</sup> However, little has been published regarding the accuracy of the method when working with line widths below 50  $\mu\text{m}$ .

We have identified in our laboratory a number of problems which arose when using designs with narrow lines.

Thin film resistors are usually designed using the following relation:

$$R = R_s \cdot n$$

where  $R_s$  is the sheet resistance expressed in  $\Omega/\square$  and  $n$  is the aspect ratio of the mask.

This relation has to be corrected in practice to take into account over-etching and undercutting effects which occur during the photolithographic etching procedures.

This paper will attempt to show a method for estimating the correction needed when employing wet chemical etching.

#### References

- (1) L.E. Murr, Microelectronics Journal 10, 4(1979)12.
- (2) H.J. Schuetze & K.E. Hennings, Solid State Technology, July(1966)31.

H - 15**HOT CARRIER INJECTION FROM ELECTROLYTE SOLUTIONS AND ITS TRANSPORT THROUGH OXIDE FILMS ON IRIDIUM AND RHODIUM.**S. Gottesfeld<sup>\*</sup>

Dept. of Chemistry, Univ. of Tel-Aviv

Oxide layers, typically 0.1-2 $\mu$  in thickness can be grown electrochemically on Iridium or Rhodium metals. Such layers serve as fast electrochromic films which switch within 10-50msec between the fully colored and fully bleached states [1-3]. In this contribution the results of measurements of carrier transport through these films will be described [4]. It will be shown that in electrochemical systems the relative electrochemical potentials of the carrier in solution and in the oxide film can be conveniently controlled by choosing the appropriate redox system (e.g. the appropriate composition of the solution). Thus, when different redox systems were employed, two very distinct modes of transport through the Ir and Rh oxide films were recorded: (1) When the redox potential was close to the Fermi level in the bleached oxide negligible transport rates were obtained. The residual current was actually due, in such cases, mainly to ionic leakage through pinholes in the film. Significant rates of charge transport could be obtained in these cases only if the applied potentials were sufficient to bring about coloration in the film. The low rates of carrier injection and transport through the bleached film are due, in such cases, to the low density and mobility of the states in the bleached oxide located near the Fermi level. (2) when the redox potential in the electrolyte was much lower than the Fermi level in the bleached form of the oxide ( $\Delta V > 500\text{mV}$ ) very high rates of hole transport through the bleached film were recorded. For electrochemical purposes the bleached film, in these last cases, acted as a perfect short. Such behaviour can be consistently interpreted in terms of hot carrier injection and transport through the "valence band" (actually a d- $\pi$  type band) of the oxide. In the band both the density and the mobility of the states are much higher, allowing very high injection and transport rates.

I.S. Gottesfeld, J.D.E. McIntyre, G. Beni and J.L. Shay,

Applied Physics Letters, 33, 208-210 (1978).2. S. Gottesfeld and J.D.E. McIntyre, J. Electrochem. Soc. 126, 742-750 (1979).3. S. Gottesfeld, J. Electrochem. Soc. 127, 272-277 (1980).

4. S. Gottesfeld, J. Electrochem. Soc., submitted.

\*Part of this work was performed during the stay of the author as a visiting scientist with Bell Laboratories, Murray Hill, N.J.

H - 16THE MEASUREMENT OF TRANSIENTS IN PHOTOELECTROCHEMICAL CELLS:  
THE EFFECT OF SURFACE ETCHING.

Z. Harzion<sup>\*</sup>, N. Croitoru<sup>\*\*</sup> and S. Gottesfeld<sup>\*</sup>  
Dept. of Chemistry<sup>\*</sup> and School of Engineering<sup>\*\*</sup>,  
The University of Tel-Aviv

The response of a photoelectrochemical cell to short light pulses is demonstrated as a tool in the study of the kinetics of the illuminated semiconductor (SC)-electrolyte (El) interface [1,2]. A well shielded spark-gap lamp served as the light source, generating pulses of 10nS width,  $5 \cdot 10^5$  watt peak power, and a continuous spectrum peaking around 3300 Å. These light pulses were directed onto the surface of a single-crystal CdSe electrode immersed in an alkaline solution containing the  $S=S^0$  redox couple. The photoelectrochemical circuit was completed by a brass counter electrode [3] of a large area. Photopotentials and photocurrent transients were evaluated after amplification with the aid of a boxcar technique. The results obtained were: (1) A pronounced effect of surface-treatment on the measured decay times could be reproducibly demonstrated, while keeping all compositions and configurational factors constant. This proved conclusively that the interfacial effects of interest are not masked by other contributions to the time-constant of the complete circuit. (2) Etching resulted in much larger (x7) photocurrent peaks with shorter (x3-x10) decay times. Traps located at the (damaged) surface are apparently responsible for a slower transfer of photocarriers through the surface of a polished electrode [4]. Such traps are removed by etching and may reform following prolonged immersion in the electrolyte, causing a renewed increase in the decay times. (3) Measured decay times under open circuit conditions ("photopotential") were >1sec, while under short circuit they were in the usec range prior to etching and in the 100nS range following etching. Hence, in this system, photocarrier decay via the external circuit (i.e. via the power-generating route) is much faster than decay by direct recombination in the SC space charge region.

1. T. Sakata and T. Kawai. Fall Meeting of the Electrochem. Soc. Los Angeles, California (1979). Extended Abs. No. 626.
2. J.H. Richardson, et al. Fall Meeting of the Electrochem. Soc. Los Angeles, California (1979). Extended Abs. No. 627.
3. G. Hodes, D. Cohen and J. Mannasen. Private Communication.
4. A. Heller, K.C. Chang and B. Miller. J. Electrochem. Soc. 124, 697 (1977).

THURSDAY MORNING, APRIL 10, 1980  
9:00

Feinberg B

## I. SEMICONDUCTORS AND MAGNETISM

H. Shaked, Nuclear Research Center, Negev-Residing

### I - 1

#### SELF-DIFFUSION PARAMETERS IN FCC METALS

L. Kornblit  
Materials Engineering Dept., Ben-Gurion University of the Negev,  
Beer-Sheva.

Migration and formation entropies, and activation volumes for vacancy self-diffusion in fcc metals are calculated with aid of an elastic continuum model. The knowledge of temperature and pressure dependence of the elastic constants of the lattice is required. The agreement between calculated and available experimental data is generally very good.

### I - 2

#### ACTIVATION ANALYSIS OF THE FORWARD -BIASED CdS- POLYSULPHIDE ELECTROLYTE SCHOTTKY BARRIER.

B. Vainas, J. Manassen, D. Cahen and G. Hodes  
Weizmann Institute of Science.

The temperature dependence of dark forward currents ( $I_f$ ) of the single-crystal CdS - polysulphide electrolyte system was studied as a function of forward bias. By plotting  $\log I_f/T^2 \cdot 1/T$  ( $T$  in  $^{\circ}K$ ), both the barrier height,  $\phi_b$ , and the preexponential factor  $A^*$  (the Richardson constant for thermionic emission) could be obtained. The  $A^*$  values were found to be bias-dependent, and decreased with increasing bias. All values of  $A^*$  were about two orders of magnitude lower than the theoretical value for CdS. Such lowering of  $A^*$  has been found for metal-insulator-semiconductor (MIS) Schottky barriers, and is due to the insulating layer formed at the interface<sup>(1)</sup>. Such an insulating layer for the CdS - polysulphide system may arise due to two separate causes. In one case, a chemical exchange between the polysulphide electrolyte and the surface of the CdS may lead to compensation of donors at the surface (e.g. by filling S-vacancies)<sup>(2)</sup> leading to a high-resistance surface layer of CdS. Also, the transfer of electrons through the Helmholtz layer of the electrolyte - CdS junction may be compared to transfer through a thin insulating region by tunneling.

The bias dependence of  $A^*$  may be expressed by a correction term,  $T_0$ , in the basic equation for thermionic emission, leading to the modified equation.

$$I_f = A^* T^2 \exp\left[-\frac{E_{act}}{k} \left(\frac{1}{T} - \frac{1}{T_0}\right)\right]$$

where  $E_{act}$  is the activation energy for the forward current  $T_0$  is the temperature at which the extrapolation of the plots of  $\log I_f/T^2$  v.  $1/T$  for different biases cross. At  $T_0$ ,  $I_f$  is independent of bias, a phenomenon known as the compensation effect. The physical nature of this effect can be rationalized assuming a linear dependence between the barrier height and the transfer of the thermally activated electrons. Large barriers are characterized by a thinner region near the surface of the semiconductor, which can result in increased probability of tunneling for the electron transfer.

#### REFERENCES

1. S. Ashok et al. Solid State Electronics, 12, 621 (1979).
2. D. Cahen et al. J. Electrochem. Soc., 125, 1623 (1978).

### 1 - 3

#### DISLOCATION-INDUCED FLICKER NOISE IN SILICON

S. Mil'shtein

Dept. of Physics, Ben-Gurion Univ. of the Negev, Beer-Sheva, Israel

This investigation was performed on n-type Si with a donor concentration of about  $10^{12} \text{cm}^{-3}$  and a dislocation density from  $10^9 \text{cm}^{-2}$  to  $10^{11} \text{cm}^{-2}$ . The first group of the specimens was mechanically deformed by a diamond indenter mounted on [111] surface under  $T=800^\circ\text{C}$ . The second group of specimens was damaged by a  $\text{CO}_2$  laser beam with an energy of about 60 joule. The dislocation clusters with density  $N = 10^9 \text{cm}^{-2} - 10^{11} \text{cm}^{-2}$  were studied by a high voltage electron microscope, which shows that most dislocations of edge type have had the Burgers vector  $\langle 220 \rangle$ . The noise spectrum detected by 3721A correlator (Hawlett Packard) shows white noise with maximum power  $A_m$  of about  $2 \cdot 10^{-12} (\text{v}^2)$  for dislocation free specimens. For the dislocated crystals  $A_m$  is of about  $3 \cdot 10^{-8} (\text{v}^2)$  and in the frequency range from 0.1 Hz to 100 Hz  $A_m$  drops like  $1/f$ . A reasonable explanation of this phenomena is due to dislocation generation-recombination activity<sup>1</sup>, which results in fluctuation of carrier lifetime:

$$\tau = \tau_0 \exp\left(\frac{q E_a}{kT}\right) \quad (1)$$

where  $E_a$  - energy of dislocation traps. Other designations have the usual meaning. In accordance to Van-der-Ziel theory<sup>2</sup> the fluctuation (1) leads to spectral density of noise:

$$S(f) = 4 \left( \frac{q \mu_p V}{L^2} \right)^2 \frac{\tau}{\Delta N^2} \frac{1}{1 + \omega^2 \tau^2} \quad (2)$$

where  $\mu_p$  - mobility of holes in the dislocated part of the crystal, which became of p-type conductivity.  $L$  - critical size of a specimen.  $V$  - is external voltage and  $\Delta N^2$  - is an autocorrelation function for concentration of carriers.

The author acknowledges the support of the US Army, research grant DAERO-78-G-115. The help of Dr.M. Mikulinsky in part of the measurements is also acknowledged.

1. T. Figielski, A. Moravski, Phys.Stat.Solidi A 6, 617 (1971).
2. A. Van-der-Ziel, in book "Noise in Measurements", J. Wiley & Sons, N.Y., 1976 p.42.

### 1 - 4

#### SCHOTTKY BARRIER EFFECTS ON THE ELECTRICAL PROPERTIES OF THE Bi-NbO<sub>2</sub>-Bi SYSTEM\*

B. Lalevic, M. Gvishi\*\*, and M. Shoga  
Department of Electrical Engineering, Rutgers University,

Transport and dielectric properties of the polycrystalline NbO<sub>2</sub> were studied in the MIM configuration as a function of the applied field, frequency and temperature. I-V-T characteristics have shown the existence of a Schottky barrier with the barrier height  $\phi_0 = 1.2$  eV which is higher than the observed thermal activation energy  $\phi_i = 0.48$  eV. Measurements of capacitance and ac conductance  $\sigma(\omega)$  have indicated that the experimental results could be satisfactorily explained by the MIM model with Schottky barriers at both metal-insulator interfaces. The functional dependence of the derived parameters such as loss tangent, real and imaginary part of dielectric constant and Cole-Cole plots is also in agreement with the above model. Deviation from this model is observed when the Schottky barrier resistance  $R_{SC}$  becomes smaller than bulk resistance  $R_b$ . For this case the Debye or the modified Debye dielectric dispersion model is found to be applicable.

\* Supported by the ARO contract

\*\* On sabbatical leave from the Israel Ministry of Defense

### 1 - 5

#### MICROWAVE CONDUCTIVITY ALONG THE SINGLE DISLOCATION IN SEMI-CONDUCTORS\*

S. Mil'shtein

Dept. of Physics, Ben-Gurion Univ. of the Negev, Beer-Sheva, Israel

The recent papers<sup>1,2</sup> present the investigation of microwave conductivity along the dislocations (MC aD) in Si and Ge. It is concluded that MCaD is due to p-type conductivity along the dislocation "core", i.e. the anomalous electrical cylinders of many dislocations are involved in collective MCaD phenomena. Unfortunately the results<sup>1,2</sup> contradict themselves and thus motivate us to analyze all the MCaD concept from first principles.

From our calculations<sup>3</sup> we find that a p-type cylinder surrounding the "core" is negligibly small at room temperature (of about  $2 \cdot 10^{-7}$  m for Ge and  $10^{-8}$  m for Si) and become larger by one order of magnitude with decreasing temperature.



On the other hand one can easily find the cylindrical skin-layer for microwaves of frequencies of about  $10^{10}$  Hz:

$$\delta = \left( \frac{2}{\omega \mu \sigma} \right)^{1/2} \quad (1)$$

where  $\omega$  - is the frequency,  $\mu$  - is magnetic permittivity of the material and  $\sigma$  - is the conductivity.

Using (1) we obtained  $\delta$  equal to  $10^{-4}$ m and  $10^{-2}$ m for Ge and Si respectively, which is much larger than even the radius of Read cylinders in those materials. Moreover, in accordance with our model of single charged dislocation the loop of two diodes will act as a very effective shunt for ultra-high frequencies. Therefore the dislocation "core" could not be involved in  $\text{MCD}$ . In order to explain the  $\text{MCD}$  we used the "Cottrell impurity atmosphere" model. The one dimensional hopping conductivity seems to be an acceptable explanation for  $\text{MCD}$  phenomena. Thus the anisotropy of microwave conductivity is caused by electrons hopping at the impurities surrounding the dislocation line.

\* Supported by US Air Force under grant AFOSR-78-3526

1. V.A. Grazhulis, V.V. Kveder, Yu. Mukhina, Yu. A. Osip'yn, Sov. Phys - JETP Lett., 24, 142 (1976).
2. Yu. A. Osip'yn, V.J. Talyansky, S.A. Shevchenko, Sov. Phys. JETP 45, 4, 810 (1977).
3. S. Mil'shtein, A. Senderichin, submitted to Phys. Rev.

## I - 6

### AN ULTRASONIC METHOD FOR THE EVALUATION OF MULTIPHASE BINARY DIFFUSION.

Z. Ronen and S. Rokhlin

Dept. of Mat. Engn., Ben-Gurion University of the Negev

M.P. Dariel

Dept. of Mat. Engn., Ben-Gurion University of the Negev and

Nuclear Research Center-Negev, Beer-Sheva, Israel.

The present communication describes the application of an ultrasonic method for the assessment of the thickness of a binary diffusion zone.

The mathematical analysis of a wave interaction with the diffusion zone shows that the amplitude and the phase of a reflected ultrasonic signal are strongly dependent on the zone parameters i.e. elastic properties and thickness. The characteristics of the reflected signal can, therefore, be used to deduce information on the diffusion zone.

In experimental part we have chosen to investigate the interaction of ultrasonic waves with the interface in Al-Cu diffusion couples. According to the phase diagram of this system, several intermetallic phases are formed at the interface of the diffusion couples. The nature

of these compound layers were examined by metallographic, scanning electron microscope and electron microprobe techniques.

Good agreement was observed between ultrasonic and direct measurements of the diffusion zone thickness. Further development of this new technique may allow its utilization for the monitoring of binary diffusion reactions.

### I - 7 INVITED

ANISOTROPIC SPIN GLASS BEHAVIOR IN  $\text{Fe}_2\text{TiO}_5$   
E. Gurewitz, Nuclear Research Center Negev

### I - 8

ISOTHERMAL ANNEALING OF A DILUTE GOLD-ERBIUM ALLOY

A. Raizman and J.T. Suss  
Solid State Physics Dept., Soreq Nuclear Research Centre, Yavne

D.N. Seidman  
Department of Materials Science and Engineering,  
Cornell University, Ithaca, NY

D. Shaltiel and V. Zevin  
The Racah Institute of Physics, The Hebrew University, Jerusalem

It was shown recently<sup>1,2</sup> that the electron paramagnetic resonance (EPR) spectrum of Er can be used as a probe to study the behaviour of defects produced by cold working in dilute Au:Er alloys. We report here an isothermal annealing study of the features of the EPR line of Er in Au, carried out in a sample prepared by rolling. We have found that the value of the residual linewidth and of the intensity of the resonance line decreased sharply, and the asymmetry parameter (A/B ratio) exhibited a peak, during the course of the annealing. This behaviour is consistent with the previously proposed concept of the segregation of erbium ions to dislocations during heating, as well as with a model describing the heated alloy in terms of two layers, each having a different effective erbium concentration (erbium ions on cubic sites), conductivity and skin depth.

1. A. Raizman, J.T. Suss, D.N. Seidman, D. Shaltiel, V. Zevin and R. Orbach, Bull. Israel Phys. Soc., 25, 43 (1979).
2. A. Raizman, J.T. Suss, D.N. Seidman, D. Shaltiel, V. Zevin and R. Orbach, J. Appl. Phys., 50, 7735 (1979).

I - 9ANTIFERRODISTORTIVE AND FERROMAGNETIC INTERACTIONS BETWEEN  $\text{Cu}^{2+}$  IONS IN  $\text{CaO}:\text{EPR}$  STUDY

J. Barak, R. Englman, A. Raizman and J.T. Suss  
Soreq Nuclear Research Centre, Yavne

The EPR spectra of pairs of  $\text{Cu}^{2+}$  ions in  $\text{CaO}$ , with  $180^\circ$  Cu-O-Cu bonds, were measured at X band and Q band. These pair centers show a strange triplet state structure: the g factor is isotropic while the fine and hyperfine structures are highly anisotropic. Also the hyperfine field parameters are different for the two ions of the pair. The spectra are discussed in terms of the static Jahn-Teller effect. It is shown that the ground state of the pair consists of a  $\theta$  orbital of one ion and an  $\epsilon$  orbital of the other. This theory is in good agreement with experiment. From the dependence of the spectra on temperature and frequency it is found that the exchange interaction between the two ions of the pair is ferromagnetic with  $|J| \sim 2 \text{ cm}^{-1}$ .

I - 10

## A NEW METHOD FOR PRECISE DETERMINATION OF SMALL CHANGES OF MÖSSBAUER LINES

E. Ratner and M. Ron  
Department of Materials Engineering, Technion, Haifa 32000, Israel

The parameters of Mössbauer resonance lines are currently determined by computer fitting of Lorentzian (or more complex) line shapes to arrays of experimental points. In order to achieve an accuracy of  $\pm 0.005 \text{ mm/sec}$  for the line position, IS (isomer shift), or line width,  $\Gamma$ , normally more than  $10^7$  counts per channel must be acquired, provided a 10% effect.

A new method of high accuracy was developed for the determination of small changes in Mössbauer parameters of the order of  $0.001 \text{ mm/sec}$  or less. Differences between two experimental sets of data points (called difference-spectra) are taken for two Mössbauer lines differing slightly in IS and  $\Gamma$ . The area of the difference-spectrum, A, was found to be related to  $\delta$ , the change in IS, and  $\Delta\Gamma$ , the change in  $\Gamma$ . Analytical expressions were derived relating the area A of the difference-spectrum to  $\delta$  and  $\Delta\Gamma$ :  $A = \phi(\delta, \Delta\Gamma)$ . The area A can be computed by general computing methods, providing a relative accuracy of the order of one percent, for  $5 \times 10^5$  counts acquired per channel with a 10% effect.

The method is adequate for the determination of small changes in Mössbauer line parameters caused by changes in temperature, applied or residual stresses, hydrostatic pressure, etc.

1 - 11**A NEUTRON DIFFRACTION STUDY OF THE DEUTERIUM  
OCCUPANCY IN  $Y_3Fe_5O_{12}D_x$** 

H. Pinto, E. Gurewitz, M.P. Dariel and H. Shaked  
Nuclear Research Center-Negev, POB 9001, Beer-Sheva

The compound  $Y_3Fe_5O_{12}$  is an oxygen stabilized rare-earth-iron intermetallic compound. It has a cubic structure with space group  $Im\bar{3}m$ [1]. These compounds display deuterium (hydrogen), sorption properties[2]. The purpose of the present work is to determine the sites occupied by deuterium in  $Y_3Fe_5O_{12}D_x$  by means of neutron diffraction. From structural considerations one expects the deuterium atoms to occupy the interstice formed by the three nearest neighbours rare earth ions. This corresponds to the 16f special position with  $x=0.28/3$ . The full occupancy of these sites would lead to a maximum uptake of 4 deuterium atoms per unit formula. Thermogravimetric determinations, however, show a maximum uptake of hydrogen close to 7 atoms per formula unit. This leads to the conclusion that the 16f site alone cannot satisfy the hydrogen occupancy requirements. Several neutron diffraction patterns of  $Y_3Fe_5O_{12}D_x$ , with  $0 \leq x \leq 4$  were taken at R.T. As x increases the appearance of a second set of reflections is observed. This set also corresponds to a bcc lattice with unit cell dimensions increased by a factor of 1.0366 with respect to the initial lattice. Line intensity calculations necessary to determine the location of the deuterium sites and their occupancy are underway.

1. M.P. Dariel and M.R. Pickus, J. Less Common Met. 50, 125 (1976).
2. M.P. Dariel, M.H. Mintz and Z. Hadari; J. de Phys. Colloque C5, suppl. au no 5, Tome 40, (1979)

I - 12

## SURFACE-SURFACE INTERACTIONS AT NANOMETER SEPARATION

J. Klein

Polymer Research Department, Weizmann Institute of Science,  
Rehovot, Israel

Interactions between surfaces and surface phases have fundamental implications in many physical and biological systems. I have designed and constructed an apparatus capable of direct measurement and characterisation of such interactions between two atomically smooth mica surfaces in a liquid. The measuring technique is based on multiple-beam interferometry, and has a resolution of 0.3-0.4 nm for surface-surface separations over the range 0-300 nm. The experimental approach permits the measurement of interactions between surface phases adsorbed onto the mica, and in this way the forces acting between adsorbed layers may be measured, as well as the nature of surface-surface interactions in a liquid medium at separations where the liquid molecular structure may be important. Preliminary results on interactions between adsorbed macromolecular surface phases are presented.

THURSDAY MORNING, APRIL 10, 1980  
9:00

Phys. Bldg.  
Small Lect.  
Hall

## J. ATOMS AND MOLECULES

B. Rosner - Israel Institute of Technology - Presiding

### J-1 INVITED

RECOMBINATION SPECTRUM OF HIGH PRESSURE XENON AND ARGON WITH Hg VAPOR

Shaul Yatsiv, The Hebrew University, Jerusalem

### J-2

SEPARATION OF  $H_2^0$  AND  $H^0+H^0$  YIELDS IN  $H_2^+$  COLLISIONS

D. Nir, S. Avraham

Technion, Israel Institute of Technology, Haifa, Israel.

The yields of the electron capture channels  $H_2^++e \rightarrow H_2^0$  and  $H_2^++e \rightarrow H^0+H^0$  are difficult to resolve because the resulting clusters are neutral and are not affected by electromagnetic fields. A fine net with small holes placed in front of the detector has been used to separate these yields. The ratio of these yields is found to be insensitive to the projectile energy in the range 100-500 keV.

### J-3

RELATIONS BETWEEN CROSS SECTIONS OF ATOMIC AND MOLECULAR PROCESSES

D. Nir

Physics Department, Technion, Haifa, Israel

The charge states of the fragments in collisions of molecular projectiles with gas targets are well described by rate equations. The solutions of these equations depend on the ratio of the charge exchange cross sections of hydrogen atom and the dissociation cross section of the molecular ion. The ratios have been extracted from the experimental data and are found to have only small dependence on the projectile energy and the gas target. This phenomenon is very helpful in predicting the charge states of molecular fragments, but still awaits explanation.

J - 4NEGATIVE FRAGMENTS YIELDS IN  $D_2^+$  COLLISIONS

D. Nir, E. Navon, B. Rosner, A. Mann

Physics Department, Technion, Haifa, Israel

We performed systematic measurements of negative fragments yields originating from  $D_2^+$  ions impinging on  $H_2$  and Ar targets. The projectile velocity was about twice the Bohr velocity (this is much smaller than in our former experiment). The negative fragment yield is found to be proportional to the square of the dissociation fraction. It seems therefore that dissociation channels containing  $D^-$  are not directly populated in  $D_2^+$  dissociation, and the  $D^-$  are coming from further collisions of the dissociation fragments.

J - 5INFRA-RED FLUORESCENCE FROM MULTIPHOTON EXCITED  $SF_6$ G. Koren, I. Levin and U.P. Oppenheim  
Department of Physics, Technion, Haifa, Israel.

Measurements of infra-red fluorescence (IRF) from  $SF_6$  gas excited by an intense pulsed TEA  $CO_2$  laser are reported. Due to the long IRF lifetime ( $\sim 1$  ms) the measurements were carried out after many collisions between the molecules of the gas had occurred. The IRF spectrum, which was recorded with a resolution of 1 to 6  $cm^{-1}$  in the frequency range of 800 to 1500  $cm^{-1}$ , showed a very strong peak shifted to the red relative to the  $\nu_3$  vibrational absorption band. The maximum shift of this peak depends on the average number of photons absorbed per molecule  $\langle n \rangle$  and we find that it equals approximately 10, 20, and 30  $cm^{-1}$  for  $\langle n \rangle = 2, 7$  and 12, respectively. The fact that the IRF near  $\nu_3$  has a strong resonance indicates that although there is a quasi-continuum of energy levels at high excitation levels, the oscillator strengths of the transitions are not uniformly distributed. The red shift observed is a result of the negative anharmonicity constants of the molecule. It is the same as the red shift obtained in  $SF_6$  gas heated thermally to the same temperature for  $3 \leq \langle n \rangle \leq 11$ . Outside this region it deviates significantly from the thermal red shift due to dissociation ( $\langle n \rangle > 11$ ) and to nonthermal energy distributions in the molecular ensemble ( $\langle n \rangle < 3$ ).

J - 6SLOW INTERMOLECULAR REDISTRIBUTION OF VIBRATIONAL ENERGY IN SF<sub>6</sub> GAS EXCITED BY A TEA CO<sub>2</sub> LASER

G. Koren, I. Levin and U.P. Oppenheim

Department of Physics, Technion, Haifa, Israel.

SF<sub>6</sub> gas was excited by the 944.2 cm<sup>-1</sup> laser line of a pulsed TEA CO<sub>2</sub> laser and the infra-red fluorescence (IRF) spectrum was measured. The laser, which emitted a parallel beam, excited a few torr of SF<sub>6</sub> gas in a specially designed absorption-fluorescence cell. The average number of photons absorbed per molecule,  $\langle n \rangle$ , was found for each laser shot by measuring the SF<sub>6</sub> absorption in the cell using calorimeters as monitors. The IRF which was emitted perpendicularly to the direction of the laser beam, was dispersed in a grating monochromator and measured by an Hg Cd Te infra-red detector. IRF spectra near the  $\nu_3$  peak were measured at intervals of 0, 0.2, 0.4, 0.6, 0.8 and 1 msec after the time of the laser excitation, and with  $\langle n \rangle \approx 1.4$ . The results show that the laser induced red shift is almost constant ( $-9 \text{ cm}^{-1}$ ) for all times measured, and that this shift is much higher than the equivalent thermal red shift ( $-5 \text{ cm}^{-1}$ ). Since intramolecular V-V relaxations are very fast (a few picoseconds to a few microseconds) and since V-T relaxations under the present experimental conditions are of the order of a few tens of microsecond-Torr, only intermolecular vibrational relaxations such as SF<sub>6</sub>(2 $\nu_3$ )+SF<sub>6</sub>  $\rightarrow$  SF<sub>6</sub>( $\nu_3$ )+SF<sub>6</sub>( $\nu_3$ ) can cause the decay of the laser excited spectrum to the thermal one. The fact that this does not happen experimentally indicates that this relaxation is slower than the 1 msec duration of the fluorescence measurement, which constitutes a lower limit to the intermolecular vibrational energy transfer rate in SF<sub>6</sub>.

J - 7COLLISIONAL PROPERTIES OF THE H<sub>2</sub> E, F  $1\sum_g^+$  STATE

D. Klügler

Racah Institute of Physics, The Hebrew University, Jerusalem, Israel

J. Bokor and C.K. Rhodes,

Department of Physics, University of Illinois at Chicago Circle, Chicago, Illinois, U.S.A.

Collisional properties of electronically excited molecular hydrogen are studied by means of selective excitation of the H<sub>2</sub> (E, F  $1\sum_g^+$ ) double minimum state. The  $v=2$  level of the inner well of the E, F state is populated by two-photon absorption of ArF\* laser radiation at 193 nm. Intracavity prisms are used to narrow the laser linewidth and tune the laser to excite single rotational



levels selectively. The population densities of the E,F ro-vibrational levels are measured by monitoring the near infrared E, F  $1\Sigma_g^+ + B 1\Sigma_u^+$  fluorescent emission. A large electronic quenching rate ( $\sim 100 \text{ \AA}^2$ ) is measured for the E, F state due to collisional transfer to the  $C_0 1\Pi_u$  state. The rotational relaxation cross sections are  $\leq 0.2 \text{ \AA}$  for  $H_2$ , but are much larger in HD ( $\sim 10 \text{ \AA}^2$ ).

## J - 8

### THE APPLICATION OF METAL VAPOR LASERS TO RAMAN SPECTROSCOPY FOR GAS AND FLAME DIAGNOSTICS.

Ilana Glatt, Israel Smilanski and Ezra Bar-Ziv  
Nuclear Research Centre-Negev, P.O.Box 9001, Beer-Sheva, Israel

Spatial distribution of concentrations and temperatures of premixed hydrogen flames were obtained from measurements of vibrational Raman spectra of oxygen, nitrogen, and water. A low cost Raman system of high performance, applying a metal vapor laser, was used.

## J - 9

### THE VALIDITY OF THE FOLDY-WOUTHUYSEN TRANSFORMATION AND VOLKOV STATES

H. Grotch and E. Kazes, Department of Physics, The Pennsylvania State University, University Park, Pa.

D.A. Owen, Department of Physics, Ben Gurion University of the Negev, Beer Sheva

We have explicitly demonstrated that the  $\vec{\sigma} \cdot \vec{B}$  term found by Kupersztych<sup>1</sup> which was thought to destroy unitarity of the Foldy-Wouthuysen transformation<sup>2</sup> has a vanishing expectation value and therefore does not contribute to the norm of the wave function of order  $1/m^2$ . This has been accomplished by using the Volkov solutions<sup>3</sup> (i. e. solutions of the Dirac equation in a plane electromagnetic field) on which we have imposed periodic boundary conditions. We have also shown that physical considerations necessitate this choice of boundary conditions.

1. J. Kupersztych, Phys. Rev. Letters 42 489 (1979)
2. L. Foldy and S. Wouthuysen, Phys. Rev. 78 29 (1950)
3. D. Volkov, Z. Phys. 94 250 (1935).

J - 10

## THE ISOELECTRONIC SEQUENCE OF NICKEL

M. Klapisch, J.L. Schwob, N. Schweitzer, A. Bar-Shalom,  
P. Mandelbaum, and B.S. Fraenkel

The Racah Institute of Physics, Hebrew University of Jerusalem

The spectra of YXII to AgXX were obtained from a high power vacuum spark and analyzed in the soft X-ray range (5-100 Å) with a high resolution grazing incidence spectrometer. Transitions  $3d^{10}-3d^9 4p$ ,  $3d^{10}-3d^9 4f$ ,  $3d^{10}-3d^9 5p$  and  $3d^{10}-3d^9 5f$  were identified. The measurements were compared with ab initio relativistic computations. The agreement is excellent. Comparison with recent results on high Z atoms by laser produced plasmas (1,2) ( $Tm^{41+}$  to  $Pt^{51+}$ ) enables to study general trends of the isoelectronic sequence.

1. A. Zigler, H. Zmora, N. Spector, M. Klapisch, J.L. Schwob and A. Bar-Shalom, J. Opt. Soc. Am. (1980, in the press).
2. A. Zigler, H. Zmora, N. Spector, M. Klapisch, J.L. Schwob and A. Bar-Shalom, Phys. Letters (January 1980).

THURSDAY MORNING, APRIL , 10, 1980  
9:00

Feinberg C

## K. APPLIED PHYSICS

G. Yekutieli, Weizmann Institute, Rehovot - Presiding

### K-1

#### LINEAR FRESNEL LENSES FOR SOLAR APPLICATIONS

E.M. Kritchman and G. Yekutieli  
Department of Nuclear Physics, Weizmann Institute of Science,  
Rehovot.

A.A. Friesem  
Department of Electronics, Weizmann Institute of Science, Rehovot.

Practical designs of linear Fresnel lenses must take into account (a) the chromatic dispersion of the lens material, and (b) the finite size of the lens grooves. Both factors are particularly important for lenses with small acceptance angle ( $\theta_0 < 5^\circ$ ). Specific designs of curved cylindrical Fresnel lenses having acceptance angles ranging from  $0.5^\circ$  to  $30^\circ$  are described. Unlike designs of idealized lenses with infinitely small grooves<sup>(1,2)</sup>, these lenses have a lower, but still impressive, concentration capability; with  $\theta_0 = \pm 0.25^\circ$  a concentration of 42 is possible. An experimental lens, of acrylic material, with  $\theta_0 = \pm 30^\circ$  was designed, built and tested. Good agreement was found between the predicted and observed performance of this lens.

(1) E.M. Kritchman et al. Solar Energy 22, 119-123 (1978).

(2) E.M. Kritchman et al. Applied Optics 18, 2688-2695 (1979).

### K-2

#### SUN TRACKERS FOR SOLAR ENERGY APPLICATIONS

M. Shachter and G. Yekutieli  
Department of Nuclear Physics, Weizmann Institute of Science,  
Rehovot.

Various solar applications like industrial heat process, thermal power generation and high concentration solar cell arrays are using solar concentrators and require special sun trackers. Several tracking systems were developed at the Weizmann Institute<sup>(1)</sup>. We shall describe and discuss here two systems: a wide angle ( $4\pi$ ) fully automatic tracker, and high accuracy small angle tracker. We shall also describe a combined system of both trackers, and a special day-cloud-night light meter that controls the operation of the tracking systems.

---

(1) Israel and USA patent.

K - 3

## ELECTRIC CIRCUIT ANALYSIS OF HIGH CONCENTRATION SOLAR CELL ARRAYS

J. Appelbaum and M. Shachter(\*)

Department of Electronic Communication, Control and Computer Systems. Tel Aviv University, Tel Aviv.

G. Yekutieli

Department of Nuclear Physics, Weizmann Institute of Science, Rehovot

Economical use of high concentration solar cell array requires the knowledge of how the array power depends on the performance of individual cells. The dispersion in the performance of individual cells may reduce the power of the array by 20% compared to total power of its individual cells. Different cells behave in a different way because of (a) non-uniformity in their production and (b) non-uniformity in cell illumination, due to misalignment of the array and tracking and concentration errors.

In this work an attempt is made to predict the power loss of the array, and to find ways to reduce it. In previous attempts it was assumed that the parameters of the individual cells in an array can be treated by a statistical model. This approach was found inadequate for high concentration arrays, or when the cell temperature is varied. In the present work a direct method is used and the performance of an array with a finite number of cells is described in terms of the measured parameters of its individual cells. Good agreement is found between experimental observations and predictions.

---

(\*)Also Department of Nuclear Physics, Weizmann Institute of Science

K - 4

## THE FADING OF DIFFERENT THERMOLUMINESCENT DOSIMETERS

B. Ben-Shachar, U. German, G. Weiser  
NRC - Negev

Recently, thermoluminescent (TL) dosimeters are used instead of films for accurate radiation exposure measurements. Their increased use is mainly due to the much wider dose range, linearity and relative small environmental influence which causes smaller fading.

The most used phosphors in personal and environmental dosimetry are the  $\text{LiF:Mg,Ti}$  and  $\text{CaF}_2:\text{Dy}$ . In most of the works published, it is accepted that the fading of  $\text{LiF}$  is about 4-8% per month (1,2,3), while the fading of  $\text{CaF}_2:\text{Dy}$  is greater and more influenced by environmental conditions (2,3). In both cases, the fading is dependent on the annealing of the phosphors

We performed measurements of fadings of both phosphors, with and without annealing, in order to learn the characteristics of the phosphors in our hatch. It will help us to correct the results of personnel and environmental dosimetry.

1. Suntharalingham, Cameron : Physics in Medicine and Biology, 13, 97-104 (1968)
2. Burghardt, Herrera, Piesch: Nuclear Instruments and Methods, 137, 41-47 (1976)
3. Burghardt, Herrera, Piesch: Nuclear Instruments and Methods, 155, 293-304 (1978)

## K - 5

### EFFECT OF INTERDIFFUSION ON THE PERFORMANCE OF $\text{PbTe-Pb}_{0.8}\text{Sn}_{0.2}\text{Te}$ IR DETECTORS

D. Eger, M. Oron, S. Rotter, N. Tamari, A. Zussman, A. Zemel and U. El-Hanany  
Soreq Nuclear Research Centre, Yavne

A systematic study of spectral responsivity, quantum efficiency, carrier concentration, zero-bias resistance and capacitance-voltage characteristics of LPE grown  $\text{PbTe-Pb}_{0.8}\text{Sn}_{0.2}\text{Te}$  heterostructure diodes is presented as a function of the  $\text{PbTe}$  growth temperature,  $420^\circ\text{C} < T < 650^\circ\text{C}$ . The results provide clear evidence for the migration of the p-n junction into the  $\text{PbTe}$  layer due to interdiffusion of native defects across the interface during  $\text{PbTe}$  growth at  $T > 480^\circ\text{C}$ . The different factors which give rise to the junction migration are discussed. The main effects of the junction migration on the diode characteristics are a reduction in the quantum efficiency at wavelengths above  $6\mu\text{m}$  and an increase in the junction zero-bias resistance. These results are interpreted on the basis of the energy band diagrams of the heterostructure diodes obtained from the capacitance-voltage characteristics and the measured carrier concentration of the epilayers. It is shown that an energy barrier for the excited electrons in the  $\text{Pb}_{0.8}\text{Sn}_{0.2}\text{Te}$  layer, formed at the  $\text{PbTe-Pb}_{0.8}\text{Sn}_{0.2}\text{Te}$  interface, is responsible for the reduction of the photosignal above  $6\mu\text{m}$ . The junction migration is completely prevented by growing the  $\text{PbTe}$  layers below  $480^\circ\text{C}$ . In this case, peak ( $\sim 10\mu\text{m}$ ) current responsivity in the range 1.7 to 2.3 A/W, quantum efficiency in the range 22 to 30% (both without an antireflection coating) and  $R_0 > 1\Omega\text{cm}^2$  are reproducibly obtained.

K - 6

**OPTIMAL CONTROL OF THERMODYNAMIC SYSTEMS OPERATING  
IN FINITE TIME**

**Yehuda B. Band, Department of Chemistry, Ben-Gurion  
University of the Negev**

**Oded Kafri, Nuclear Research Center-Negev**

**Peter Salamon, Department of Chemistry, Tel-Aviv  
University, and Departments of Mathematics and Chemistry,  
Arizona State University, Tampe, Arizona.**

Using optimal control theory we determine the solution of the prototype problem: Given a finite amount of time, what is the optimal motion of a piston, fitted to a cylinder containing a gas which is pumped with a given heating rate and which is coupled to a heat bath. The optimal motion is such as to maximize the work obtained via the piston in a specified period of time. Explicit thermodynamic analyses of the solutions are carried out for various examples. The efficiency, and the gain over non-optimal paths, are studied. Significant improvement over the bound on the efficiency as calculated by (infinite time, reversible) thermodynamics is obtained. The nature of the limit of the optimal solution as the time approaches infinity is determined. For a finite heating rate the optimal path is irreversible even as the time approaches infinity.

Thursday Afternoon

14:30 PLENARY SESSION II

G. Goldring, The Weizmann Institute - Presiding

T. Banks, The Tel Aviv University

UNIFIED THEORIES OF ELEMENTARY PARTICLE  
INTERACTIONS (40 min.)

COFFEE BREAK

E. Kogan, Tadiran Electronics Division, Holon

SURFACE ACOUSTIC WAVES TECHNOLOGY AND ITS  
APPLICATIONS TO SIGNAL PROCESSING IN  
COMMUNICATION SYSTEMS (40 min.)

## AUTHOR INDEX

- ACHIAM Y., F-2  
 ADMON U., H-1  
 ALSTER J., A-1  
 AMIT M., D-11  
 APPELBAUM J., K-3  
 ARAD B., A-11, G-5  
 ARAUJO C.B. DE , D-13  
 ARIELI R., D-2  
 AVISHAI Y., A-2  
 AVNI Y., B-1, B-3  
 AVRAHAM S., J-2  
 AZBEL M. YA., C-5, C-9, F-4  
  
 BAND Y.B., K-6  
 BANKS T., PLENARY II  
 BAR V., B-2  
 BARAK J., I-9  
 BAR-NOY T., G-7, G-8  
 BAR-SHALOM A., J-10  
 BAR-TOUV J., A-8  
 BAR-ZIV E., J-8  
 BATTISTUZZI G., A-10  
 BAUMEL S., C-2  
 BEN-ABRAHAM S.I., F-9  
 BEN-SHACHAR B., K-4  
 BENSIMON D., D-4  
 BERAN M.J., D-14, D-15  
 BERANT Z., A-6  
 BERGMAN A., C-3  
 BERGMAN D.J., C-13, D-18  
 BERNSTEIN W., E-5  
 BIRENBAUM Y. A-6  
 BLAUGRUND A.E., G-3  
 BOKOR J., J-7  
 BOXMAN R.L., E-8, E-9  
 BRODY M., C-6  
 BROUDE C., A-9  
 BURDE J., A-5  
  
 CAHEN D., H-3, H-12, I-2  
 CARMEL Y., E-10, E-11  
 CROITORU N., H-11, H-16  
 CUPERMAN S., E-3, E-4, E-5, E-6,  
 E-7  
  
 DANA I., B-9  
 DANINO M., C-8  
 DARIEL M.P., H-4, I-6, I-11  
 DAYAN M., H-11  
 DEUTSCHER G., C-4, H-6, H-10, H-13  
 DOSTROVSKY I., PLENARY I  
 DRYER M., E-6  
 DWIR B., C-4  
  
 EGER D., K-5  
 EHRENFREUND E., C-1  
 EL-HANANY, U., K-5  
 ELIEZER S., A-11, G-5  
 ENGLANDER A., D-4  
 ENGLMAN R., I-9  
 EREZ G., D-11, D-17  
 EYLON S., E-10, E-11  
  
 FRAENKEL B.S., J-10  
 FREUND I., D-12  
 FRIESEM A.A., D-3, D-6, K-1  
  
 GABAY S., D-10, D-17  
 GERMAN U., K-4  
 GINZBURG A., E-10, E-11  
 GITERMAN M., F-5, F-7, F-12, F-14  
 GIVON M., G-10  
 GLATT I., J-8  
 GOLDSMITH S., E-8, E-9  
 GOMBEROFF L., E-2, E-7  
 GOREN Y., E-10, E-11  
 GOTTESFELD S., H-15, H-16  
 GREENFIELD A.J., C-11  
 GROTCHE H., J-9  
 GUR J., D-5  
 GUREWITZ E., I-7, I-11  
 GURVITZ S.A., A-3  
 GVISHI M., I-4



HALPERN V., C-2, C-10  
 HARDY A., D-1, D-16  
 HARPAZ A., B-4  
 HARZION Z., H-16  
 HASPEL M., H-14  
 HASS M., A-9  
 HAVAZELET D., G-6  
 HODES G., H-3, H-12, I-2  
 HOROWITZ B., C-7  
 HULEIHIL KH., B-7

JACOB I., A-12  
 JACKEL S., G-4, G-5  
 JANAI M., H-8, H-9

KAFRI O., K-6  
 KAHANE S., A-6  
 KAPITULNIK A., H-6  
 KATZIR A., D-2, D-6, D-7  
 KAPON E., D-7  
 KAVEH M., C-3, C-6, C-8  
 KAWADE K., A-10  
 KAZES E., J-9  
 KAZINETS M.M., H-2  
 KEDMI Y., D-8  
 KERSZBERG M., F-3  
 KLAPISCH M., J-10  
 KLEIN J., I-12  
 KLIGLER D., J-7  
 KOGAN E., PLENARY II  
 KOREN G., J-5, J-6  
 KORNBLIT L., I-1  
 KOVNER I., B-5  
 KRITCHMAN E.M., K-1  
 KRUMBEIN A.D., G-5

LABATON I., A-5  
 LACOUR-GAYET P., C-13  
 LALEVIC B., I-4  
 LAVI S., D-9, D-11, D-17  
 LAWIN H., A-10  
 LEIBOWITZ E., B-8  
 LEREAH Y., H-11  
 LEVIN I., J-5, J-6  
 LEVIN K., H-9  
 LEVUSH B., E-3  
 LEVY U., D-3  
 LINSKY D., F-10  
 LOEBENSTEIN H.M., G-4, G-5  
 LOTEM H., D-13

MALIN S., B-7  
 MANASSEN J., H-3, H-12, I-2  
 MANDELBAUM P., J-10  
 MANN A., J-4  
 MARON Y., G-2, G-3  
 MILGROM M., B-5  
 MIL'SHTEIN S., I-3, I-5  
 MINZ M.H., A-12  
 MIROE E., D-11, D-17  
 MIROVSKY Y., H-12  
 MIZUTANI T., A-2  
 MOALEM A., A-4, A-5, A-8  
 MOREH R., A-6  
 MUKAMEL D., F-3, F-6

NAVON E., J-4  
 NIR D., J-2, J-3, J-4  
 NIV Y., A-9

OPPENHEIM U.P., J-5, J-6  
 OREG J., G-9  
 ORON M., K-5  
 OWEN D.A., J-9

PAISS Y., A-11  
 PALEVSKI A., H-10  
 PELED A., H-14  
 PERETSMAN L., F-13  
 PETRAN F., E-4  
 PINTO H., I-11  
 POLTURAK E., F-11  
 PRATT B., H-9

RAIZMAN A., I-8, I-9  
 RAPPAPORT M.L., H-6, H-10, H-13  
 RATNER E., I-10  
 RHODES C.K., J-7  
 RICHTER V., A-5  
 ROKHLIN S., I-6  
 RON A., F-1  
 RON M., I-10  
 RONEN Z., I-5  
 ROSEN N., PLENARY I  
 ROSENBAUM R., F-11  
 ROSENFELD Y., G-10, G-11  
 ROSNER B., J-4  
 ROTH I., E-5  
 ROTH S., D-12  
 ROTTER S., K-5  
 ROZENFELD S., A-4

SALAMON P. K-6  
 SALZMANN D., G-5  
 SAPIR M., G-8  
 SCHILLER N., B-3  
 SCHINDEWOLF U., F-10  
 SCHLESINGER Y., C-2  
 SCHWEITZER N., J-10  
 SCHWOB J.L., J-10  
 SEGALOV Z., E-10, E-11  
 SEIDMAN D.N., I-8  
 SHACHTER M., K-2, K-3  
 SHAHAL O., A-12  
 SHAHAM J., B-6  
 SHAKED H., I-11  
 SHALEV S., E-8, E-9  
 SHALOM E., G-1  
 SHALTIEL D., I-8  
 SHAMIR J., H-7  
 SHAPIRA M., C-2  
 SHARON B., D-6  
 SHIKHMANTER L., H-4  
 SHNIDMAN Y., F-6  
 SHOGA M., I-4  
 SHTRIKMAN H., H-5  
 SHTRIKMAN S., D-4  
 SHVARTS D., G-6, G-7, G-8, G-9  
 SINVANI M., C-11  
 SISTEMICH K. A-10  
 SLATKINE M., D-4  
 SMILANSKI I., D-9, D-10, D-17,  
 J-8  
 STEINBERG V., F-7, F-8, F-10,  
 F-12, F-13, F-14  
 STRAUSS M., G-9  
 STROUD D., D-18  
 SUSS J.T., I-8, I-9  
 SVERBILOVA T., F-13  
 SZAPIRO S., H-5  
  
 TALIANKER M., H-4  
 TAMARI N., H-5, K-5  
 TENENBAUM J., D-9  
 TENNE R., H-3, H-12  
 THIEBERGER R., G-10  
 TREVES D., D-4, D-8  
 TSERRUYA I., A-7  
 TUR M., D-14, D-15  
  
 VAGNER I.D., C-12  
 VAINAS B., I-2  
 VIRMONT J., G-7  
 VORONEL A., F-10, F-13  
  
 WEIL R.B., H-9  
 WEISER G., K-4  
 WEISS I., E-6  
 WISER N., C-3, C-6, C-8  
 WOLF A., A-6, A-10, A-12  
  
 YATSIV S., J-1  
 YEKUTIELI G., K-1, K-2, K-3  
  
 ZEMEL A., A-9, K-5  
 ZEVIN V., I-8  
 ZIGLER A., G-4, G-5  
 ZINAMON Z., E-1  
 ZMORA H., G-4, G-5  
 ZUSSMAN A., K-5  
 ZWEIGENBAUM S., G-4, G-5